UNCLASSIFIED

AD 418599

DEFENSE DOCUMENTATION CENTER

FOR

SCIENTIFIC AND TECHNICAL INFORMATION

CAMERON STATION, ALEXANDRIA, VIRGINIA

UNCLASSIFIED

NOTICE: When government or other drawings, specifications or other data are used for any purpose other than in connection with a definitely related government procurement operation, the U. S. Government thereby incurs no responsibility, nor any obligation whatsoever; and the fact that the Government may have formulated, furnished, or in any way supplied the said drawings, specifications, or other data is not to be regarded by implication or otherwise as in any manner licensing the holder or any other person or corporation, or conveying any rights or permission to manufacture, use or sell any patented invention that may in any way be related thereto.

VERTICAL DIFFUSION FROM AN ELEVATED LINE SOURCE OVER A VARIETY OF TERRAINS

Part A
Final Report

to

Dugway Proving Ground

Contract DA-42-007-CML-545

by

T. B. Smith
M. A. Wolf

March 31, 1963

Meteorology Research, Inc.
2420 North Lake Avenue
Altadena, California

MR163 FR-71

TABLE OF CONTENTS

	Page
SUMMARY	i
I. INTRODUCTION	1
A. Background	1
B. Objectives	1
C. Test Sites	2
D. Scope	2
II. OPERATIONS	4
A. General	4
B. Tracer System	4
1. Tracer	4
2. Dissemination	5
3. Sampling	6
C. Meteorological Instrumentation	6
1. Surface	6
a. Turbulence	6
b. Temperature	7
c. Wind Velocity	7
2. Airborne	8
a. Turbulence	8
b. Temperature	8
III. DIFFUSION CONSIDERATIONS	9
A. Application of Dallas Model	9
B. Estimation of i_e	10
1. Stability Factor	10
2. 100-Foot Turbulence	10
3. Release Height Turbulence	10
IV. TEST ANALYSES	12
A. Oklahoma	12
1. Terrain Description	12
2. Meteorological Environment	12
3. Estimation of Effective Turbulence	13
4. Analysis of Results	14
B. Texas	16
1. Terrain Description	16
2. Meteorological Environment	16
3. Estimation of Effective Turbulence	17
4. Analysis of Results	18
C. Washington	20
1. Terrain Description	20
2. Meteorological Environment	20
3. Estimation of Effective Turbulence	22
4. Analysis of Results	22

		Page
	D. Nevada	24
	1. Terrain Description	24
	2. Meteorological Environment	24
	3. Estimation of Effective Turbulence	26
	4. Analysis of Results	27
V.	DISCUSSION OF RESULTS	31
	A. Terrain Comparisons	31
	1. Elevation-Relief Ratio	31
	2. Grain and Relief	32
	B. Turbulence Comparisons	33
	C. Dosage Models	34
VI.	CONCLUSIONS	37
VII.	RECOMMENDATIONS	38
VIII.	ACKNOWLEDGMENTS	39
	REFERENCES	40
	APPENDIX A - COMPARISON OF ROTOROD AND FILTER SAMPLERS	A-1
	APPENDIX B - AIRCRAFT TURBULENCE MEASUREMENTS	B-1
	APPENDIX C - DATA SUMMARY	C-1

SUMMARY

A series of 36 diffusion trials were conducted in four widely differing terrains and meteorological regimes. Objective of the program was to extend the results obtained in the Dallas Tower Program to other terrain and meteorological conditions.

Instrumentation at each site included a 100-foot portable tower equipped to measure turbulence, temperature, and winds. This tower was usually located near the center of a 25-mile rotorod sampling line. Two 30-foot meteorological towers were generally located near the ends of the sampler line. FP tracer material in a line source was released from an aircraft flying crosswind and slightly upwind of the beginning of the sampler line. In addition to accomplishing the FP dissemination, the aircraft recorded temperature, turbulence, and several other parameters in order to extend the observation network upward and in order to determine inhomogeneities in these parameters along the sampler line. Pibals taken at the 100-foot tower location completed the observational program.

Three techniques for estimating effective turbulence values between the ground and release height were developed for use in the present program. These techniques were based on Dallas Tower data for which measurements of turbulence and correlated variables were available. One of the techniques required the use of a stability factor, formed from the vertical change in potential temperature from ground to release height and a mean wind speed. A second technique estimated effective turbulence from a direct measurement of turbulence at the 100-foot level. A third technique provided the estimate from a direct measurement of turbulence at release height.

Results from the northeastern Oklahoma site indicated that observed ground dosages were closely related to computed dosages, using the Dallas ground dosage model, if effective turbulence was estimated from measured turbulence at release height. Due to turbulence inhomogeneities along the sampler line, the stability factor and 100-foot turbulence techniques did not give effective turbulence estimates which were representative of the early stages of cloud travel.

In the Corpus Christi, Texas area the cloud arrived at the ground from the elevated release much more rapidly than could be explained on the basis of turbulent mixing processes. Some type of organized flow pattern, displacing the center of the cloud downward, must be called upon to explain the observed dosages. It is suggested that this flow pattern is of a helical form, oriented along the mean wind and similar to that previously observed by Woodcock and used by Hallanger to explain diffusion data obtained some time ago at Camp Cooke, California.

At the Washington site, safe flying restrictions caused the release height to be about 1200 feet above the sampler line. Turbulence values during the night were not sufficiently large to bring the cloud to the ground in quantity. In two afternoon trials, added turbulence due to convection resulted in moderate ground dosages. Additional data of interest were obtained by instrumenting Steptoe Butte with rotorod samplers. Larger dosages were observed on the lee slope of the butte but dosages even on top of the butte were frequently very small in spite of the release height being the same elevation as the top.

The Nevada trials were conducted along a sampling line which covered the windward and leeward slopes of an extensive 1000-foot ridge. Releases were made around 10 miles upwind of and 400 feet above the crest of the ridge. Substantial dosages were observed on the lee slope due to extensive downslope flow in the lee of the ridge. Under stable, nocturnal conditions the center of the cloud was carried upward on the windward slope after release and the cloud material had little chance to enter the drainage flow on this slope. Dosages observed on this slope during the trials apparently resulted from lateral flow into the sampler line in drainage from a nearby higher mountain peak.

Results of the trials brought out clearly 1) the importance of additional understanding of small-scale organized flows which displace the center of the cloud from a straight line path, and 2) the need for a dosage prediction technique capable of use under typical, inhomogeneous turbulence conditions.

I. INTRODUCTION

A. Background

A study of the vertical diffusion of an elevated line source particulate cloud was initiated in 1961 to obtain a quantitative relation between observed ground dosages and measured meteorological parameters (1). In that study, 37 releases of fluorescent particle tracer (FP) were made by an L-23 aircraft in crosswind traverses upwind of the 1420-foot TV tower located at Cedar Hill, Texas. Release heights varied between 380 and 1050 feet above the tower base.

Measurements of FP dosage distributions were made in the horizontal for 30 miles downwind of release and frequently on a 25-mile crosswind line located about 25 miles downwind of the release. Dosage measurements in the vertical were made at intervals of 50 to 150 feet on the TV tower.

Wind velocity and temperature were measured at 12 levels on the tower and, at five of these levels, bivanes were used to measure the vertical component of atmospheric turbulence. At one of the bivane levels the horizontal component of turbulence was measured.

Analysis of the resulting data was based on the relationship between turbulence characteristics and diffusion which has been established by the Porton group in England (2, 3). It was shown that, despite significant variations which require further investigation, there was good agreement in the first 10 - 15 miles between the observed dosage and the dosage predicted by the conventional diffusion equations modified for direct use of the turbulence measurements.

Further, it was demonstrated that a stability factor involving only air temperatures and wind speeds could be used for an approximate determination of the turbulence parameter involved in the prediction technique.

The applicability of this dosage prediction technique to other areas where terrain, mean wind, or stability differ from the Cedar Hill area was the immediate concern at the conclusion of the initial study.

B Objectives

The primary objective of this study is the applicability of the dosage prediction technique of the Dallas Tower study under the differing conditions of other areas. In addition, several means for estimation of the appropriate turbulence parameter in these areas have been examined.

Careful examination of the test data should explain any observed inconsistencies with the Dallas model and contribute to the formulation of a more general model.

C. Test Sites

In the selection of test sites for diffusion studies of this scale there are several requirements which, in order to reduce the complexities of field operations, are common to all. It is necessary that adverse weather conditions such as rain, fog, low clouds, and extreme wind speed or variable wind direction, which might limit ground or aircraft operations, be of minimum occurrence. Existing roads parallel to the persistent wind direction are necessary for the FP sampling. Special requirements for each site are dictated by the particular features which are to be investigated.

Two sites, in Oklahoma and Washington, were selected on the basis that their homogeneous rolling terrain provides greater surface roughness than the Dallas area. The homogeneity is necessary to minimize the influence of crosswind variations on the dosage distribution. The two sites differ somewhat in their relief with the Washington area having the higher, more frequent undulation. Although uniformly low vegetation characterizes the Washington area, the Oklahoma area has a wide variety of vegetation. A further consideration in the relative diffusion associated with these two areas is the stability of the air mass. The modified maritime air of Oklahoma coupled with only moderate surface cooling at night produces less stable nocturnal conditions there than in Washington.

The two other sites were selected for their single-featured interest. The Texas site on the Gulf Coast offers a flat coast line normal to the wind flow. The Nevada site presents a crosswind ridge superimposed on an otherwise rather smooth surface in the immediate vicinity. These features which impose a downwind variation in turbulence are of particular interest in the evaluation of a model which includes only vertical turbulence variations.

The four sites which are located in Fig. 1 are described in more detail in Section IV.

D. Scope

At each of the four test sites, 7 to 9 successful releases of FP were made from an Aero Commander airplane which made a crosswind traverse slightly upwind of the rotorod sampling line.

The surface measurement network of each area consisted of the FP sampling system and the meteorological instrumentation. Sampling was done by rotorod collectors extending, at one-mile intervals, downwind

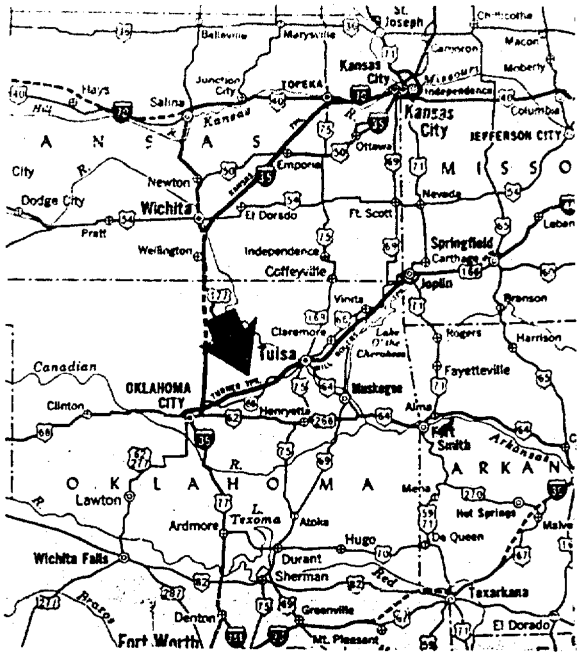

OKLAHOMA

TEXAS

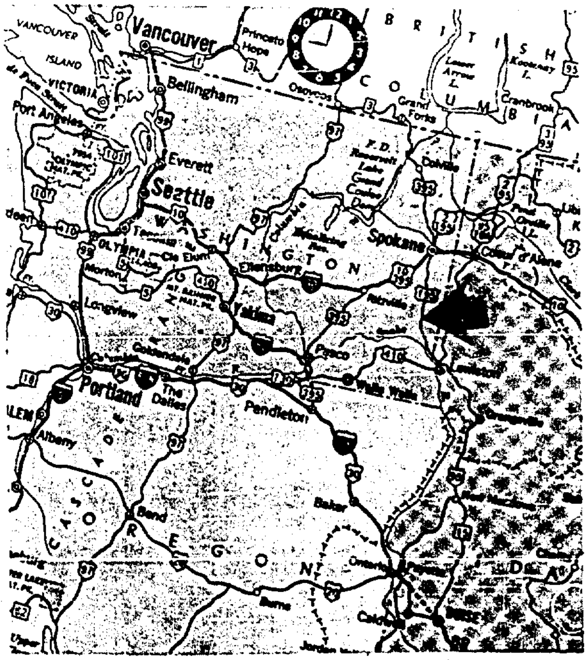

WASHINGTON

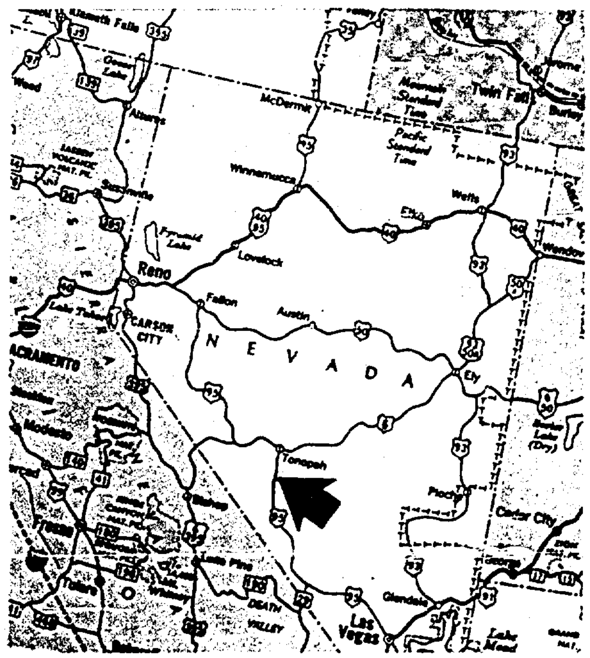

NEVADA

TEST SITE LOCATIONS

Fig. 1

along a 25-mile line from a short distance upwind of the expected initial touchdown of the tracer. Measurements of wind velocity, temperature, and turbulence were made at three tower locations (30 feet, 100 feet, and 30 feet heights) along the sampling line.

The aircraft was instrumented to extend the surface measurements in the vertical. In addition, the airplane provided a means for determining significant horizontal variations of the meteorological parameters.

Single-theodolite pibals provided the wind velocities required to complete the vertical profile. Wherever possible, the local USWB-FAA offices were contacted to facilitate operational scheduling. Synoptic data were collected from the USWB office at Los Angeles International Airport for use in the analysis phase.

A total of 36 releases were made; three were unsuccessful. Test 10, which had a disseminator malfunction, and Tests 20 and 34, which were unsuccessful due to wind shift associated with frontal passages, will not be discussed further. Twenty-eight of the successful tests were conducted after sundown and the other five, at least one in each area, in the afternoon. The results of these 33 tests are detailed in this report.

II. OPERATIONS

A. General

Master Control was located in the instrument trailer at the 100-foot tower site. This was the base for all surface operations. The base for aircraft operations was a nearby airport. Communications between the two were maintained by telephone. When airborne, communications were made with VHF radio.

Two FM radio-equipped vehicles were regularly available for servicing the rotorod samplers and the 30-foot towers. The FM radio at Master Control completed the communications network.

The aircrew was composed of a pilot and an observer who were responsible for maintenance and operation of the aircraft, the disseminator, and the airborne instrumentation.

The surface operation required a three-man crew: the operations director, the field engineer, and the rotorod serviceman.

B. Tracer System

1. Tracer

The aerosol tracer used in this investigation was zinc-cadmium sulfide containing one per cent by weight of micronized Valdron Estersil for increased fluidity. The property of this substance to [illegible] tion and facilitates visual assessment of dosage on the collectors.

Lot 14, produced in November 1959 by U. S. Radium Corporation, was used for all tests. Table I presents the evaluation of this lot. It is seen that the size of particles will assure a negligible settling rate in an investigation of this scale.

TABLE I

INSPECTION REPORT: ZINC-CADMIUM SULFIDE

Particle Size Range	% (By Number) in Each Size Range
0.00 - .47	.97
.47 - .66	.78
.66 - .93	1.75
.93 - 1.32	4.95
1.32 - 1.87	15.42
1.87 - 2.64	36.57
2.64 - 3.73	33.85
3.73 - 5.27	4.17
5.27 - 7.45	1.46

Mean particle count: 2.16×10^{10} per gram.

2. Dissemination

Dissemination was accomplished with a disseminator furnished by DPG. Since this disseminator was similar to the one used in the Dallas tests, the same dissemination efficiency (39%) was assumed.

The metered flow of FP was adjusted for a rate of 1.5 pounds per mile to achieve a source line length of 30 miles. The release rate and length of line were optimized for the total FP drum content of 50 pounds to provide measurable particle recovery and to reduce the effects of edge dilution along the sampling line. The standard source strength, Q , including the disseminator efficiency, was determined to be 1.11×10^{9} particles/ft.

The crosswind, dissemination traverse passed upwind of the rotorod sampling line with approximately 15 miles of source line extending on either side. Only at the Texas site can the release height above the terrain be clearly stated, for at the other three sites the terrain itself is quite variable in elevation. The range of elevations in Washington and Nevada prevented operation of the aircraft as low as would have been desired. In fact, the releases in Washington were nearly 1000 feet above the highest rotorod sampler and the release height in Nevada was between 400 and 1400 feet above the samplers. In Oklahoma the separations between release and samplers ranged from 300 to 600 feet. The height above samplers in Texas was 500 feet except for Tests 15 and 17 which were 750 and 1000 feet, respectively.

3. Sampling

The primary FP aerosol collector was the battery-powered rotorod sampler furnished by DPG. Collection of the FP is affected by impaction on two vertical rods coated with silicone grease, which are rotated at 2400 rpm. The theoretical sampling rate for the geometry and rotational speed of this sampler is 41.8 liters/min. Comparative tests during the present program of the rotorod sampler and the filter sampler, operated with an assumed 100% efficiency at 6.5 liters/min. indicate an efficiency of about 75% as shown in Appendix A. The effective sampling rate of the rotorod sampler used in the previous Dallas Tower study for the calculation of total dosage was 33 liters/min. While Appendix A of this report shows the somewhat lower average value of 30.8 liters/min. the individual values are too variable to warrant a change. Therefore, the value of 33 liters/min. is used herein.

Samplers were spaced downwind of the release line, at approximately one-mile intervals alongside the road, from a short distance upwind of the anticipated initial position of FP touchdown for about 25 miles. Three of the rotorod locations were at the three tower locations. At the 100-foot tower, in addition to the surface sampler at the standard five-foot height, samplers were operated at 30 and 100 feet to determine the degree of mixing in this layer.

Rotorods were activated well ahead of the expected arrival of the FP and were operated for a sufficient period to insure passage of the cloud.

Particle assessment was performed at Utah State University under contract from DPG. The total counts were determined manually with recounting of a random sample by a different person as an error evaluation. Examination of the dual counts reveals that, on the average, they differ from their mean by less than 5%.

C. Meteorological Instrumentation

1. Surface

a. Turbulence

Turbulence measurements were made at the three tower sites with the MRI bivanes described in the previous report (1). At the 100-foot tower the vertical and horizontal components of turbulence at 10, 30, and 100 feet were recorded on magnetic tape together with a time signal for subsequent sigma evaluation. Simultaneously, a recording of the three vertical and 100-foot horizontal components were made on the paper tape of a modified two-channel Brush

recorder in order that turbulence measurements could be monitored for test operation criteria.

The sigma analysis of the taped signal was performed in Altadena with the sigma meter described in the previous report which has been modified slightly to provide sampling times of 2-1/2, 5, 15, 30, and 180 seconds.

Bivanes were also located at the 30-foot levels of the two 30-foot towers. Portable sigma meters provided continuous records of sigma at these locations on spring-driven Esterline-Angus recorders. A sampling time of 24 seconds was used for the portable sigma meters.

b. Temperature

Shielded, thermistor temperature sensors were located at the 10, 30, and 100-foot levels of the 100-foot tower and at the 10 and 30-foot levels of the 30-foot towers to provide temperature profiles. At all locations, the temperature traces of these quick-response sensors were recorded on one channel of the two-channel, spring-driven Esterline-Angus recorders. At the 30-foot towers, the two temperatures and 30-foot wind direction were cycled to give a sample of all three quantities every ten minutes, while at the 100-foot tower the three temperatures were cycled over the same period of time. In order to have instantaneous temperature differences at the 100-foot tower, the recorder was modified prior to the Washington and Nevada tests so that the 30-foot temperature, the temperature difference between the 100-foot and 30-foot levels, and the temperature difference between the 10-foot and 30-foot levels were alternately recorded during each ten-minute cycle.

c. Wind Velocity

Wind speeds from the two levels of the 30-foot towers and the three levels of the 100-foot tower were recorded with the side-marker pens of the Esterline-Angus recorders. Three cup anemometers were used as the wind speed sensors.

Wind direction was measured by the bivanes at their locations. As previously noted, the wind direction measurements at the 30-foot tower sites were recorded alternately with the temperatures on the Esterline-Angus recorders. The main tower recordings of the horizontal turbulence component provide the wind direction information there since the bivanes were properly oriented in the horizontal.

An extension to the vertical profile of the wind velocity was provided by a single theodolite pibal to approximately 3000 feet above the surface at the 100-foot tower site. These observations were made within the hour following FP release.

Wet bulb-dry bulb readings with a sling psychrometer and altimeter settings with an aircraft altimeter were recorded periodically throughout each test period at the 100-foot tower site.

2. Airborne

a. Turbulence

Three types of turbulence measurement were available in the aircraft instrument package: rate-of-climb, accelerometer, and the MRI turbulence meter. The first two have the disadvantage that they include the aircraft and pilot responses to turbulence. These responses are difficult to remove from the turbulence record and, as a consequence, low frequency turbulent energy (large eddy sizes) is not often measured from aircraft. The turbulence meter which is described in detail in Appendix B measures the important smaller eddies through the response of a propeller, mounted in the airstream, to longitudinal variations in the air speed. The recorded signal can be calibrated as a function of the rate of dissipation of turbulent energy, $\dot{\varepsilon}$, and is intimately related to the turbulence parameter σ. It is possible therefore to extend surface measurements of turbulence to greater elevations and to determine the existence and magnitude of horizontal variations.

b. Temperature

The thermistor temperature system was similar to the surface units. The sensor was located within a stagnation housing mounted in the airstream. Due to the dynamic heating of the air the indicated temperatures require a correction which is proportional to the square of the airspeed. The exact correction which is subtracted from the indicated value is $\lambda(V/100)^2$ where V, the aircraft velocity is in mph and λ is a recovery factor determined to be 0.91.

III. DIFFUSION CONSIDERATIONS

A. Application of Dallas Model

Results of the Dallas Tower studies suggested that ground dosage from an elevated line source could be adequately described within the first 10 to 15 miles by a slight modification of the standard line source formula to the form:

$$D = \frac{2Q}{3i_e^2 \times U\sqrt{2\pi}} \, e^{\frac{-H^2}{18 i_e^4 x^2}} \qquad (1)$$

Where D is the ground dosage at a distance x from the release, U is wind velocity, H is release height, Q is the source strength, and i_e is an "effective" turbulence value, representing a weighted average of the turbulence between the ground and the release height. In calculating this average the regions of low turbulence (near release height) are given greater weight since the cloud spends a greater portion of its travel time in these layers and passes through the higher turbulence regions much more quickly. The equation above assumes the validity of the cluster diffusion growth equation:

$$\frac{d\sigma}{dx} = 3i^2 \qquad (2)$$

recently proposed by Hay-Smith (7).

Two primary problems arose in applying Eq. (1) to the Dallas Tower data:

1) The diffusing cloud grows in a region of inhomogeneous turbulence. An average or "effective" turbulence value can only approximate the true growth conditions over a limited range of downwind distances.

2) At some distance downwind, the linear growth rate of the cloud, given by Eq. (2), no longer holds and the cloud enters a somewhat slower growth regime. According to Pasquill (4), this decrease in growth rate occurs at a downwind distance of roughly 50 times the existing scale of turbulence.

In the Dallas data and in the data to be discussed in the present report, the problems resulting from an inhomogeneous turbulent distribution occur at an earlier stage in the cloud growth and hence assume greater importance.

In addition to these problems, inherent in using an "effective" turbulence value, application of the Dallas model to other areas requires a method for obtaining an estimate of the "effective" turbulence value between the ground and release height when direct measurements of turbulence on a 1400-foot TV tower are not available. Three methods for accomplishing this are described in the following section.

B. Estimation of i_e

Effective turbulence values, i_e, have been computed from the Dallas data for various release heights such as 450, 750, and 1050 feet. It is then necessary to consider what simple, observable meteorological parameters may be used to estimate these effective values in the absence of actual turbulence measurements from the ground to release height.

1. Stability Factor

The first system for estimating effective turbulence has been shown in the report covering the Dallas Tower studies. It has been suggested that the stability factor:

$$S.\ F. = \frac{\Delta\theta}{\bar{u}^2}$$

where $\Delta\theta$ and $\bar{u}$ represent the potential temperature change and average wind between ground and release height, is a useful indicator of effective turbulence in the same layer. Graphs showing these relationships for the various release heights are shown in Fig. 2. It is to be noted that the relationships are most clearly established for release heights in the 450 and 750-foot categories.

2. 100-foot Turbulence

Since the present studies include tower turbulence measurements to 100 feet, it is useful to consider to what extent effective turbulence can be estimated merely from knowledge of the 100-foot turbulence value. Fig. 3 shows these relationships in the Dallas data for various release heights. It is seen that the predictability of i_e becomes increasingly difficult for higher release heights. Other factors such as temperature differences and turbulence profiles in the lowest 100 feet were added to the prediction system shown in Fig. 3, but little improvement was noted and it is apparent that most of the variability in i_e is described by the 100-foot turbulence value alone.

3. Release Height Turbulence

It has been possible during the present program to obtain a measure of the turbulence at release height from measurements made

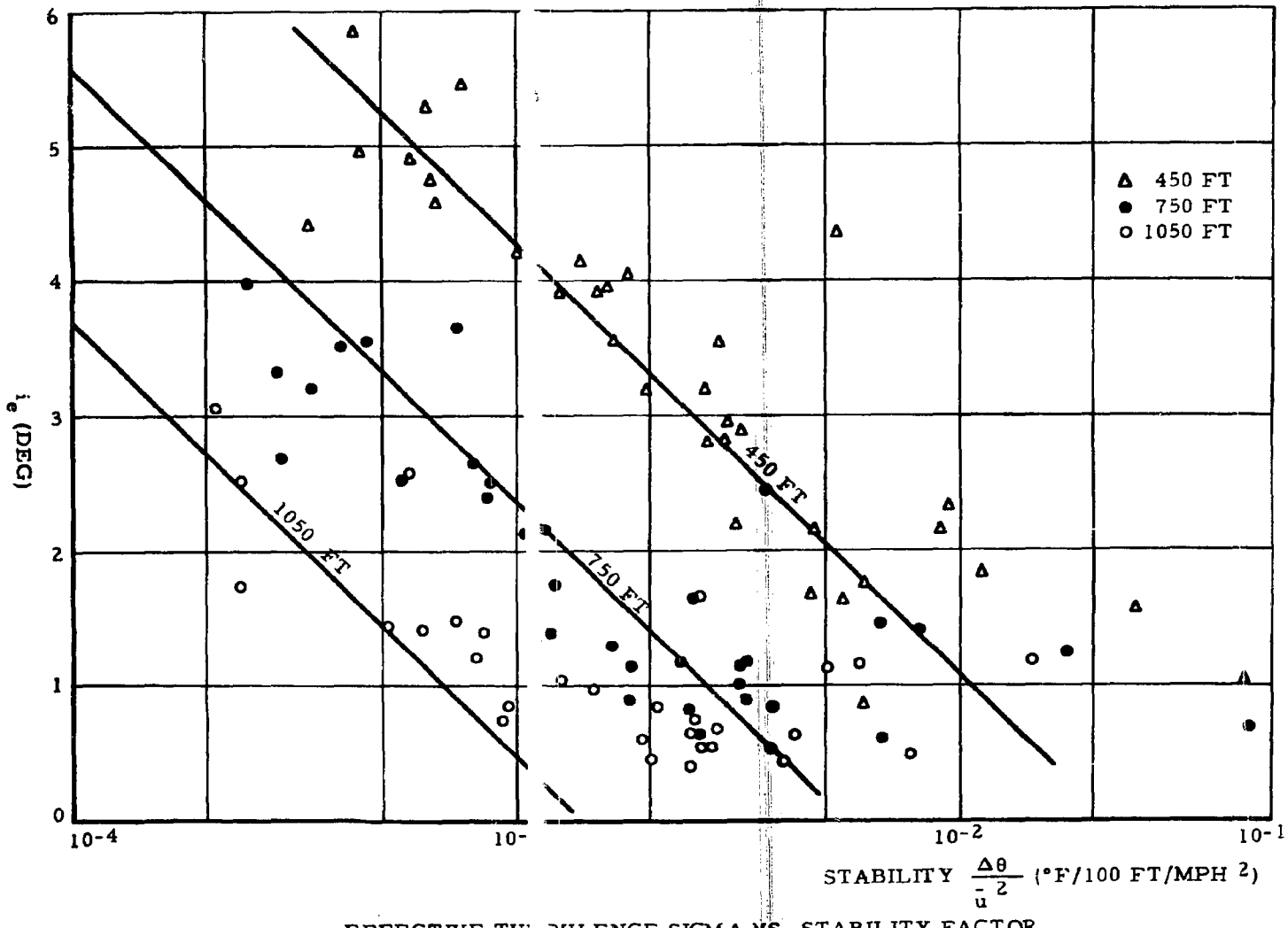

EFFECTIVE TURBULENCE SIGMA VS. STABILITY FACTOR

Fig. 2

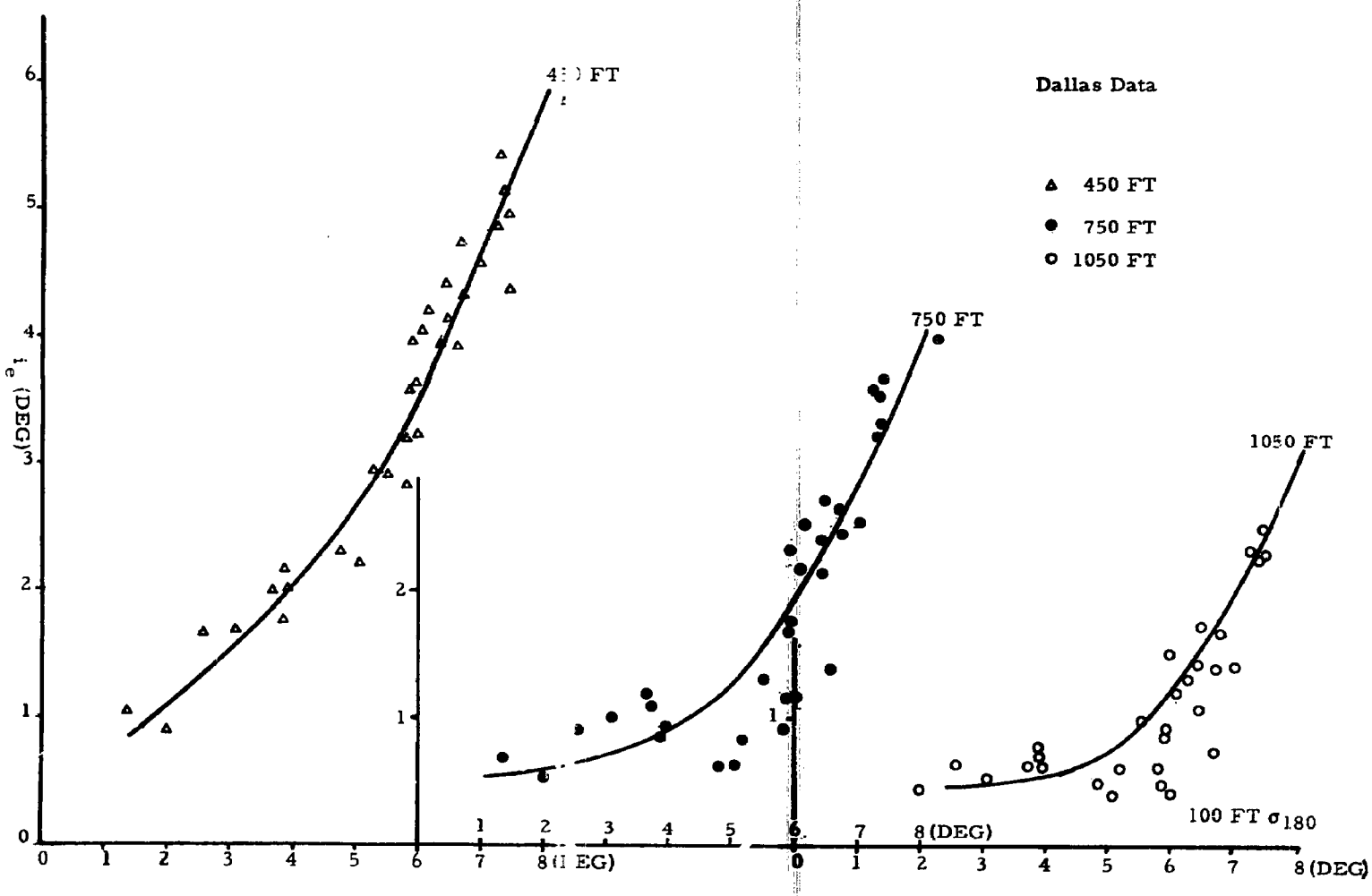

Fig. 3. EFFECTIVE TURBULENCE VS 100 FT TURBULENCE

by the MRI turbulence meter in the aircraft. This instrument essentially responds to ambient turbulent energy in a narrow frequency band within a frequency range high enough for the aircraft response to the turbulence itself to be neglected. A true, undistorted measure of turbulent energy can thus be obtained in the defined frequency band. Through knowledge of the turbulent energy at these high frequencies and through the additional input of ambient wind at release height (pibal wind), it is possible to calculate σ_5, the turbulence value corresponding to a 5-second sampling period. Details of this relationship are shown in Appendix B.

For many diffusion problems, knowledge of turbulence values for longer sampling periods or knowledge of the actual turbulence spectrum itself might be considered essential. The aircraft, with the present instrumentation, provides only a turbulence value at the high frequency end of the turbulent energy spectrum. In nighttime situations this value will comprise a considerable portion of the total energy spectrum. In daytime regimes, convection introduces additional low frequency energy and the aircraft will measure a smaller proportion of the total spectrum.

For the present study, Dallas Tower data for σ_5 at release height have been plotted against effective turbulence, i_e, in Fig. 4. As might be expected, measured turbulence at release height becomes an increasingly important predictive factor for higher release elevations.

The preceding three systems for estimating effective turbulence, i_e, are available for use in the analysis of the present program. It should be expected that the systems might not apply as well in other terrain and

In rougher terrain, for example, turbulent energy in the lower layers might be expected to be greater than in the Dallas data for similar conditions of vertical wind and temperature profiles. To demonstrate these limitations, the three systems are applied wherever possible to the present data and discrepancies in observed and predicted dosages are explained in terms of physical deviations from the Dallas model.

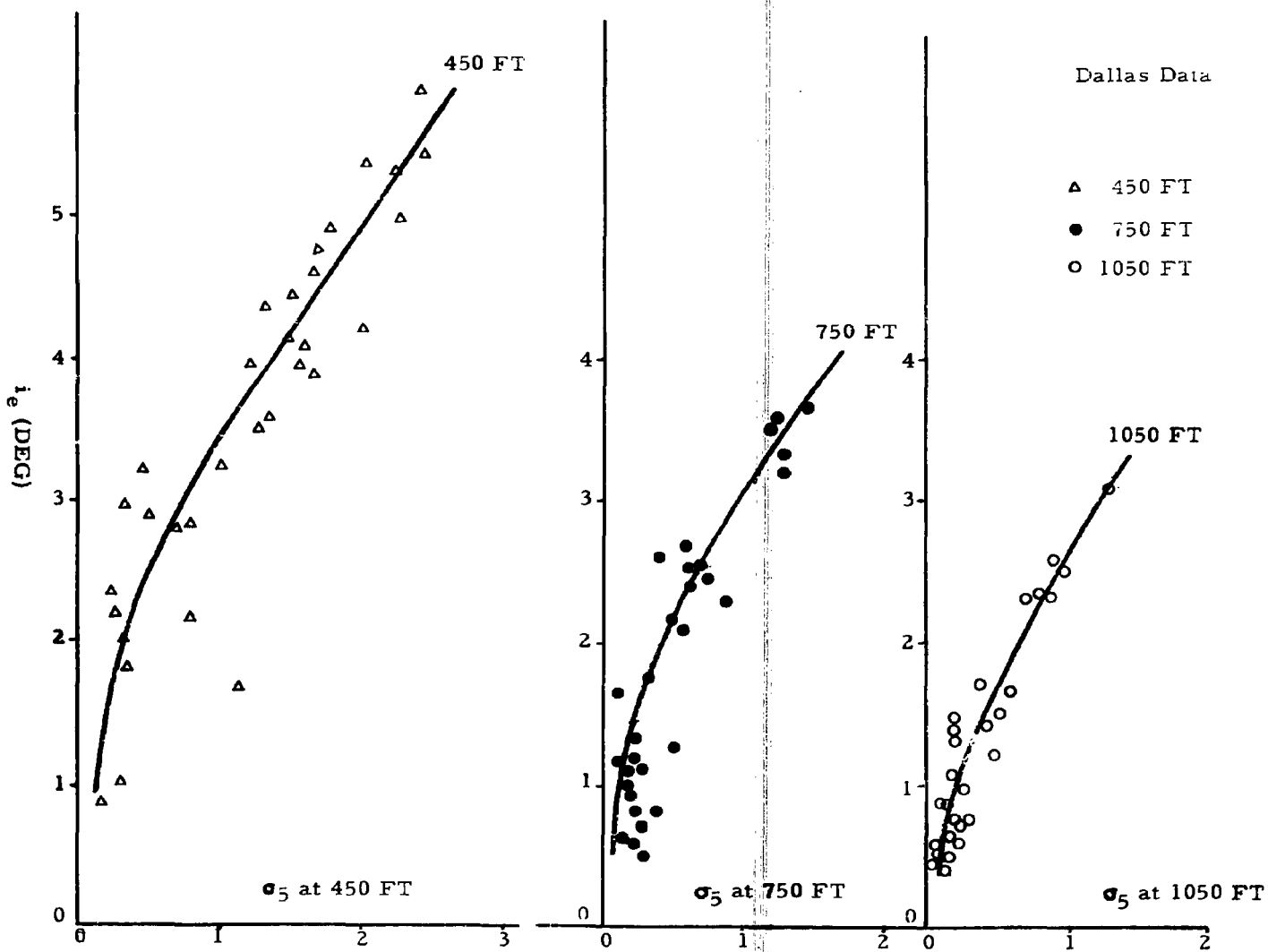

Fig 4. EFFECTIVE TURBULENCE VS σ_5 AT RELEASE HEIGHT

IV. TEST ANALYSES

A. Oklahoma

1. Terrain Description

Fig. 5 shows an elevation contour map of the Oklahoma site. A 25-mile north-south rotorod sampling line extends from near Cushing to Pawnee, crossing the Cimarron River. The area is characterized by rolling terrain of rather shallow amplitude with ridges spaced on the order of 5 miles or more apart. Elevations in the general area range from slightly less than 800 feet to near 1100 feet.

The elevation profile along the sampler line is shown in Fig. 6. The principal terrain features along the line are the low elevations near the Cimarron River generally increasing to near the end of the sampler line. Tower locations are shown in Fig. 6 at the appropriate points along the line.

Also shown in Fig. 6 is a typical turbulence record made during Trial 2 in the aircraft during a flight at 1400 feet MSL (approximately 500 feet above ground) over the sampler line. The effect of the increased roughness north of the Cimarron River on the turbulence along the sampler line is clearly shown. This change in turbulence during the downwind passage of the cloud along the line is of significance in the subsequent analysis and will be referred to later.

2. Meteorological Environment

Oklahoma tests were conducted during the period June 4-17, 1962 in typical summer, southerly flow conditions. The nearest low pressure trough or low center was generally present in western Kansas or eastern Colorado.

These synoptic conditions are similar to those prevailing during a majority of the Dallas Tower tests. Under these conditions a low level wind jet commonly forms at night as the wind aloft increases as a result of the decrease in the afternoon surface heating. Fig. 7 shows the generation of the low level jet during the nighttime hours of the Oklahoma test period. The wind profiles were drawn from a composite of all pibal measurements made during the test period for the hours shown.

It has been shown previously in the Project Windsoc studies that the wind shear existing between the surface and the center of the low level jet is frequently sufficient to overcome the temperature stability forces in these layers. As a result, turbulence is generated throughout most of the lowest 1000 - 1500 feet. This is substantially verified

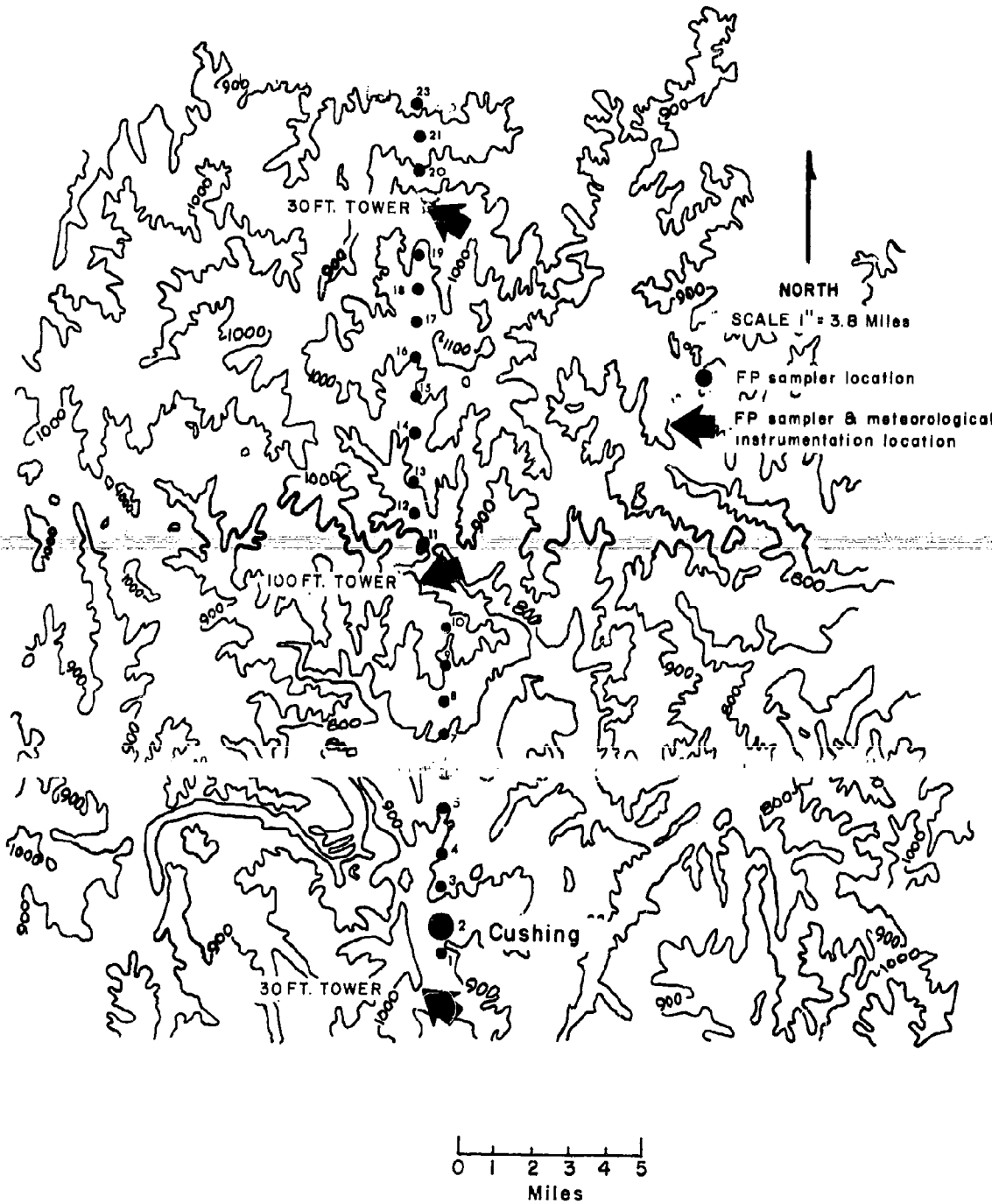

OKLAHOMA TEST SITE

Fig. 5

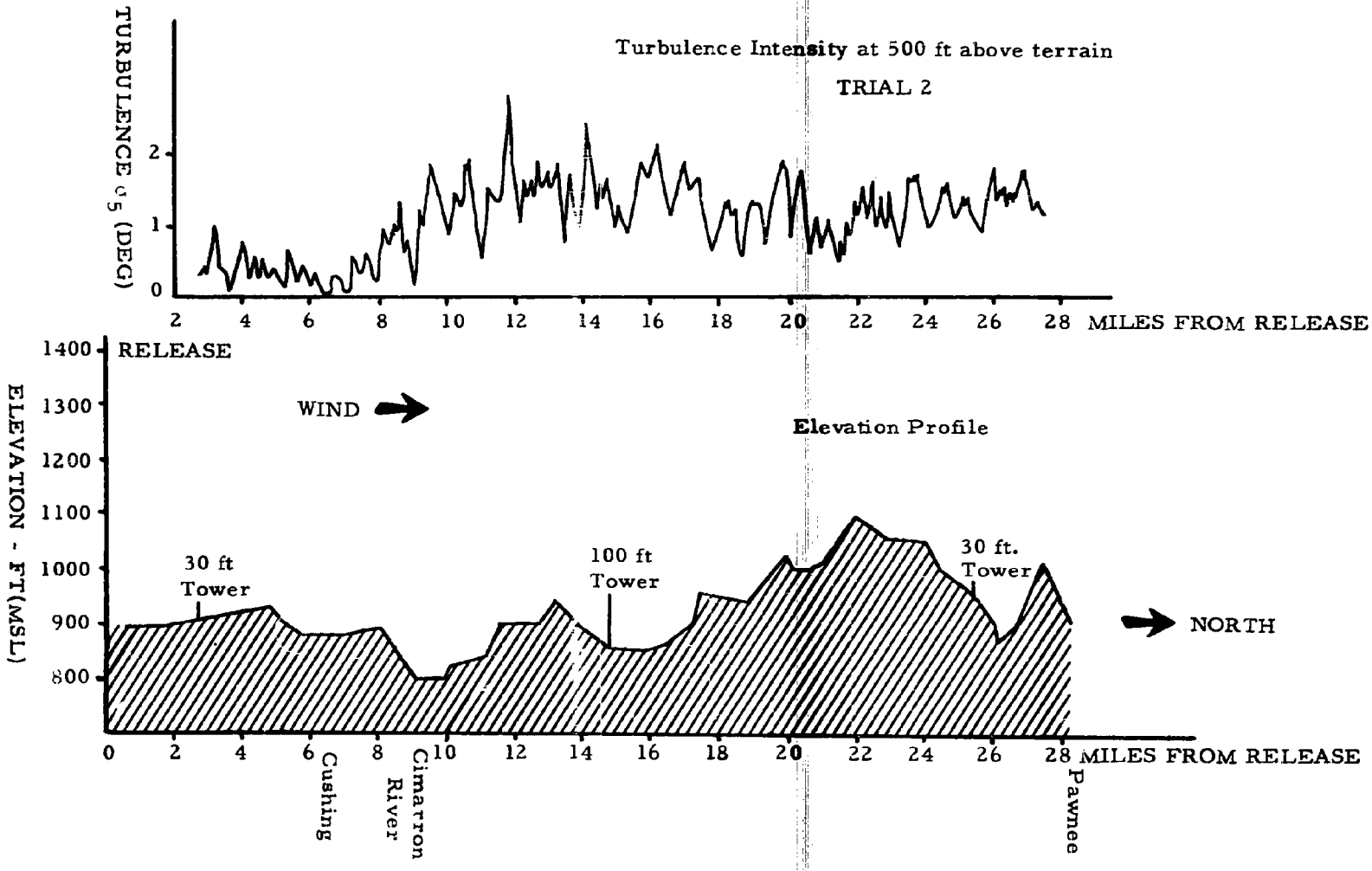

Fig. 6. OKLAHOMA DIFFUSION TEST SITE

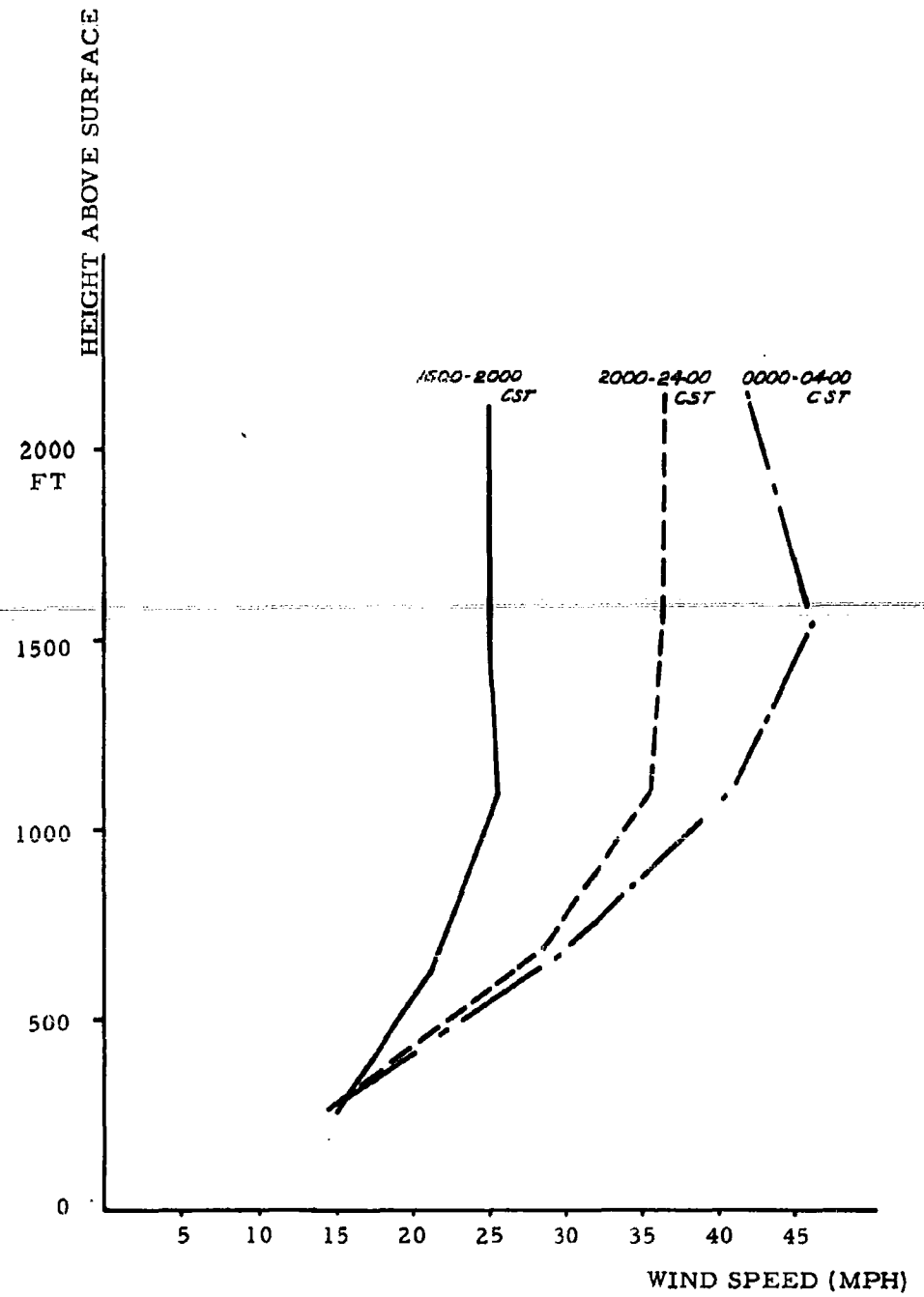

AVERAGE WIND PROFILE - OKLAHOMA

Fig. 7

by vertical aircraft soundings of turbulence in the Oklahoma tests which showed little or no turbulence above 1000 to 1300 feet in any of the trials.

The conclusion is reached, therefore, that the Oklahoma releases were made within the well developed turbulence layer associated with the low level jet in conditions comparable to those normally found in the Dallas area. Upward growth of the cloud would be expected to occur to a level of 1000 - 1500 feet but would be limited thereafter by the low turbulence levels near and above the center of the jet.

One of the trials during the Oklahoma series (Trial 4) deserves further mention as being somewhat different from the above picture. Winds aloft and at the ground were lighter than the remainder of the trials and there was insufficient vertical wind shear to cause significant turbulence in the layers near release height. Supporting evidence of this lack of turbulence comes from Richardson number calculations (ground to release height) which show a value of .77 for Trial 4 compared to less than .3 for all other Oklahoma trials. As a consequence of this lack of wind shear, effective turbulence values for this trial are significantly lower than any other in the Oklahoma test series.

3. Estimation of Effective Turbulence

The turbulence intensity profile shown in Fig. 6 is characteristic of most of the trials at the Oklahoma site. Turbulence at release height was generally lower in the region south of the Cimarron River than along the sampler line to the north of the river. Under these conditions in the early stages of cloud travel the environment turbulence, as shown in Fig. 6, was relatively low and cloud growth would be small. Increased turbulence north of the Cimarron River was generally not a factor in bringing the cloud to the ground more rapidly since cloud touchdown occurred upwind of the river (except Trial 4).

Table II shows effective turbulence values (i_e) computed by each of the three methods mentioned in an earlier section:

TABLE II

EFFECTIVE TURBULENCE - OKLAHOMA

Trial	Stability Factor ($\Delta\theta/\bar{u}^2$)	100-Foot Turbulence	Release Height Turbulence
1	---*	5.8 DEG.	2.85 DEG.
2	3.5 DEG.	9.0	2.65
3	5.4	6.0	1.5
4	1.9	2.2	.8
5	4.1	4.7	2.3
6	3.5	5.8	2.95
7	3.2	7.2	3.0
8	5.0	4.6	3.2
9	3.7	5.4	2.85

*$\Delta\theta$ negative

Effective turbulence values in Table II calculated from the 100-foot turbulence values are seen to be generally larger than those obtained by the other methods. This apparently is the result of the general situation shown in Fig. 6, i.e., the 100-foot tower was located in a region of relatively high turbulence and is not representative of conditions during the early part of the cloud travel.

Effective turbulence values calculated from the stability factor are also considerably larger than those obtained from aircraft turbulence measurements at release height. Wind surface and temperature data for the stability factor calculations were taken at the location of the 100-foot tower and these calculations also appear to reflect the increased turbulence regime north of the Cimarron River.

The turbulence measured at release height during the dissemination run consequently appears to be the most representative value for computations of cloud growth in the critical early stages of cloud travel.

4. Analysis of Results

Ground dosage calculations have been made for all of the Oklahoma trials using aircraft measured turbulence values and average winds between ground and release height. Specific values of the parameters for each trial are shown in Appendix C. Dosages were calculated from Eq. (1) given in an earlier section.

Fig. 8 shows a comparison of calculated and observed ground dosages for all of the Oklahoma trials. Agreement is considered to be generally good and comparable to the agreement previously obtained between calculated and observed dosages in the Dallas data.

No calculated dosage is shown for Trial 4 since calculated amounts were inconsequential at all downwind distances. (Note the effective turbulence level of .8 degrees.) The indications from the observed ground dosage amounts are that no substantial amount of the cloud arrived at the ground until some 17 miles downwind. At this stage in the cloud travel (just north of the 100-foot tower in Fig. 6) the terrain rises rather sharply and the cloud arrived at the ground in large amounts only in this higher terrain. Trial 4 is thus considered as a case of marked downwind inhomogeneity in the effective turbulence values.

It is useful to compute ground dosages on the basis of a box model which assumes a uniformly mixed cloud from the ground to the top of the turbulent layer. Depth of the turbulent layer is obtained from aircraft soundings. Results of these calculations are shown in Table III.

TABLE III

BOX MODEL COMPUTATIONS

Trial	Depth of Turbulent Layer	Wind Velocity	Dosage ($\frac{\text{part-min}}{\text{liter}}$)
1	1000 ft	15 mph	29.7
2	900	17	29.1
3	1200	15	24.8
4	1000	13	34.3
5	1000	12	37.2
6	1200	13	28.6
7	1200	15	24.8
8	1000	17	26.3
9	1300	16	21.4

Comparison of the box model computations with observed ground dosages shows that the box model values are approximated in each trial after a downwind travel distance of around 15 miles. Thereafter the box model serves as an adequate estimate of ground dosage. This suggests that vertical growth of the cloud, after 15 miles or so, is primarily controlled by the boundary limits of the turbulent layer and the system of relating vertical growth to a single "effective" turbulence value is likely to be useful mainly in the first 10 to 15 miles of travel.

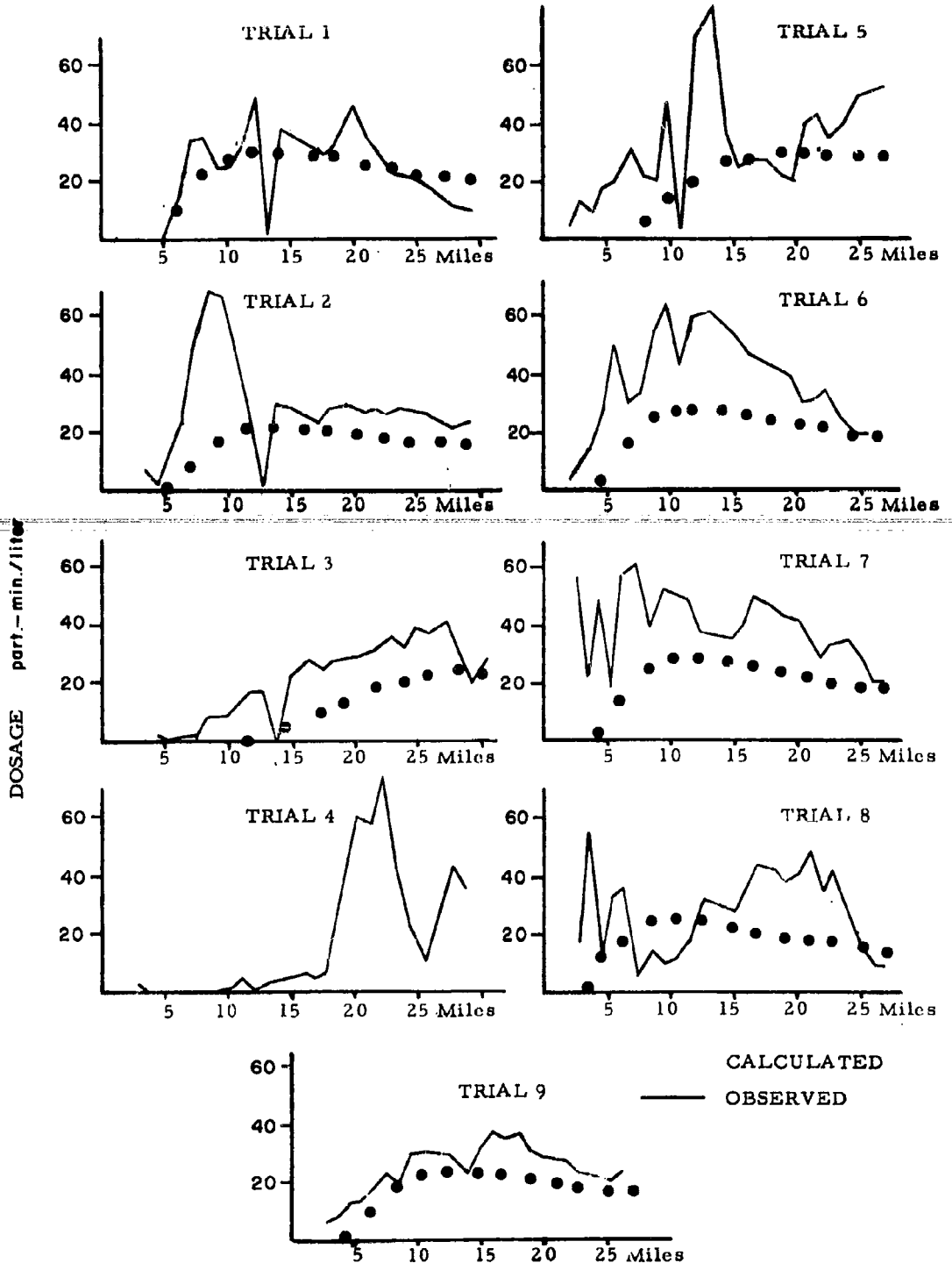

Fig. 8 OKLAHOMA DOSAGES

B. Texas

1. Terrain Description

A series of nine trials were conducted during the period of June 24-30, 1962 in the vicinity of Corpus Christi, Texas, Fig. 9 shows a map of the coastline and rotorod sampling line at the Texas site. In this area the coastline extends in a northeast-southwest direction. Paralleling the main coastline and about 6 - 7 miles seaward is a narrow island which is partially connected by causeway to the mainland near Port Aransas. The sampling line extended from Port Aransas along the causeway to the mainland and thence northwestward to the vicinity of Taft. One of the 30-foot towers was located near the beach of Port Aransas and the other inland at Gregory. The 100-foot tower was located on the mainland coastline at Aransas Pass. FP releases were made offshore from Port Aransas along a line parallel to the coastline and 1 - 6 miles offshore.

Inland from Aransas Pass the terrain is extremely flat with no distinguishing features. Ground roughness increases at Port Aransas and to some extent at Aransas Pass as air passes from the smooth water surface over the slightly rougher coastal land and inhabited area. However, the ground roughness throughout the entire test area is much less than prevails near Dallas or at the Oklahoma site.

2. Meteorological Environment

During the test series in late June south to southeasterly flow conditions were present in the Corpus Christi area. In contrast to the Dallas and Oklahoma areas, a low level wind jet did not develop during the night under the conditions observed. This undoubtedly results in part from the small diurnal temperature changes on the coast (about 6°F vs. 11°F change inland at Gregory). Due to the limited heat sources during the afternoon on the coast, convection does not exert much effect in slowing down winds aloft during the afternoon and the small nocturnal cooling does not permit much change in the turbulence regime during the night. Composite wind profiles from pibals taken at Aransas Pass during the test series show relatively constant winds throughout the range of hours represented. These wind profiles are shown in Fig. 10.

The ocean in the Corpus Christi area is a warm water region with surface temperatures in the low eighties during the test period. The steady supply of heat from the water surface results in near adiabatic temperature lapse rates in the lowest 1000 - 1500 feet during the late afternoon. During the night, however, slightly stable conditions generally develop even though the surface temperature decrease is small.

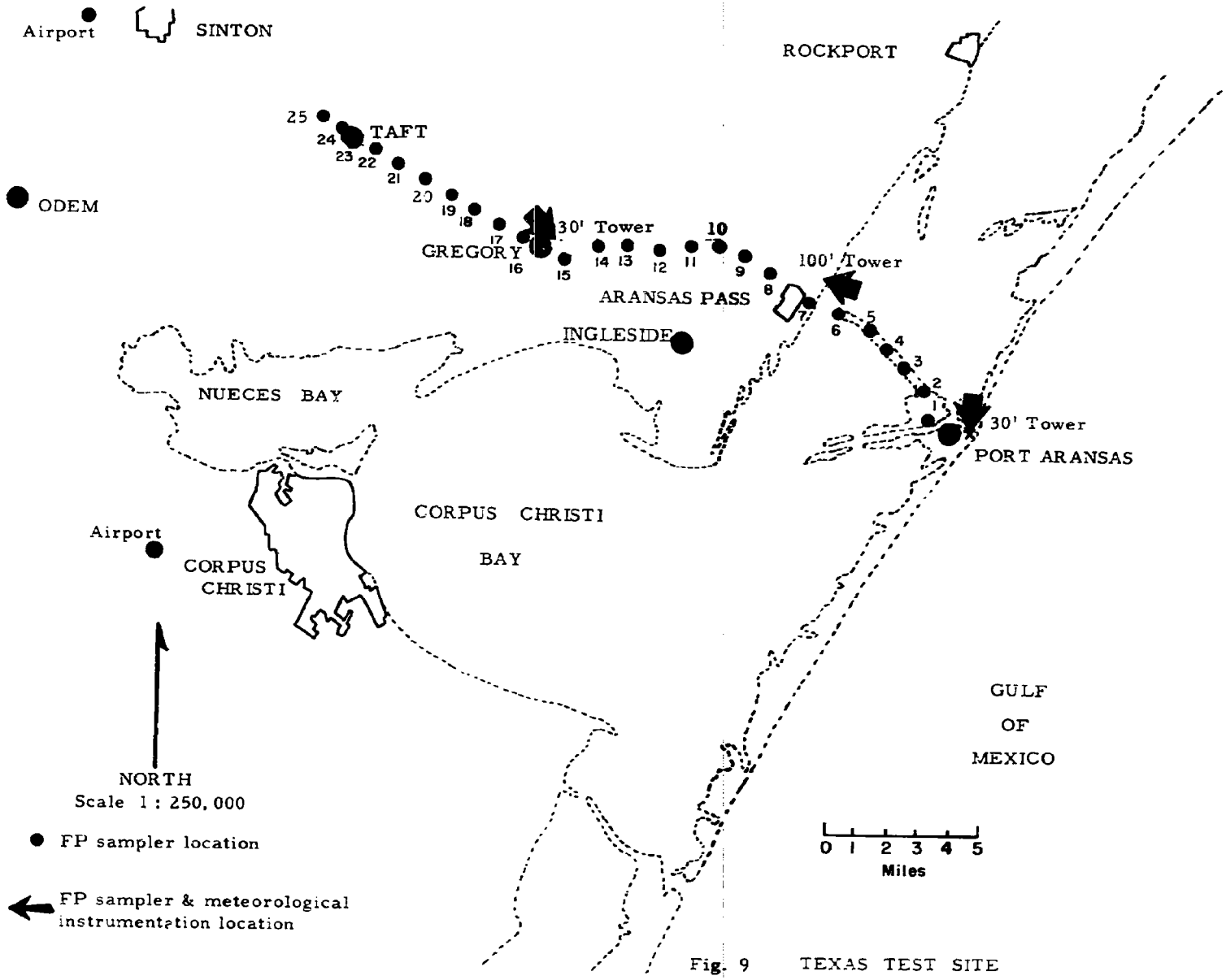

Fig. 9 TEXAS TEST SITE

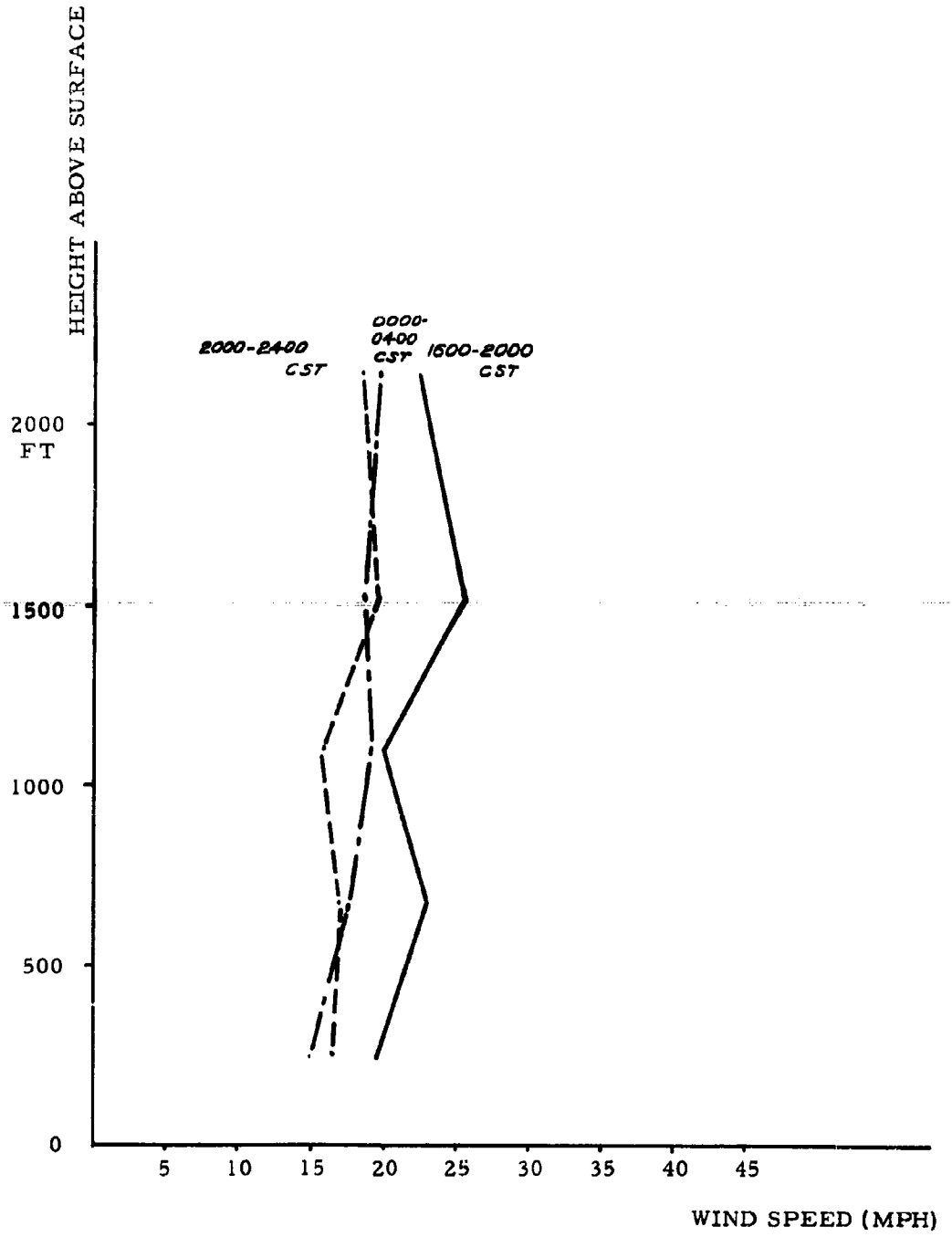

AVERAGE WIND PROFILE - TEXAS

Fig. 10

Turbulence values in the Corpus Christi area were small at all levels compared to the Oklahoma and Dallas areas. Even though the vertical temperature stability is not great, the input of turbulent energy at the ground surface is small due to the general lack of roughness.

3. Estimation of Effective Turbulence

Effective turbulence values have been obtained for the Corpus Christi trials by each of the three methods described in an earlier section. These values are shown in Table III:

TABLE III

EFFECTIVE TURBULENCE - TEXAS

Trial	Release Height	Stability Factor ($\Delta\theta/\bar{u}^2$)	100-Foot Turbulence	Release Height Turbulence
11	500 FT	---*	1.6 DEG.	1.3 DEG.
12	500	---*	2.1	1.4
13	500	4.7 DEG.	1.8	1.0
14	500	6.1	1.2	1.2
15	750	5.1	.85	1.1
16	500	3.1	2.0	1.2
17	1000	1.5	1.0	.85
18	500	3.1	4.2	1.3
19	500	2.9	3.8	1.6

*Negative $\Delta\theta$

It is to be seen from the above table that effective turbulence values calculated from 100-foot turbulence observations and those calculated from aircraft turbulence observations are in reasonable agreement. In general, the aircraft data appear to yield a slightly smaller value of effective turbulence which suggests that the vertical distribution of turbulence may be somewhat different in the Corpus Christi region than usually found in the Dallas area, i. e., the turbulence decreases somewhat more rapidly from the surface upward to 500 feet than normally is the case at Dallas.

Effective turbulence values obtained from the stability factor method are considerably larger than found from the other two methods and, in addition, there appears to be little correlation between the stability factor values and others. This feature is apparently the result of the smooth terrain conditions and the lack of turbulent energy input at the surface levels in Corpus Christi. Given a certain roughness

of the terrain, such as at Dallas, ($\bar{u}^2$) represents a measure of the turbulent energy introduced in the low levels by the ground roughness. $\Delta\theta$ represents the extent to which temperature forces tend to damp out the turbulence. In an area such as Corpus Christi with a smaller degree of roughness the same value of $\bar{u}^2$ creates somewhat less turbulent energy input and a given value of $\Delta\theta/\bar{u}^2$ should be associated with a lower turbulent energy level. Use of the Dallas $\Delta\theta/\bar{u}^2$ vs. turbulence relation thus tends to overestimate turbulent conditions in Corpus Christi and leads to values as shown in Table III. This table points out the inherent advantages of direct measurements of turbulence over the use of temperature profile-wind velocity factors in the estimate of effective turbulence.

In view of the relatively good agreement of 100-foot turbulence and release height turbulence estimates in Table III and the results of the preceding study in Oklahoma, estimates of the effective turbulence from aircraft data have been used in the following section.

4. Analysis of Results

Observed dosages for the various Texas trials are shown in Fig. 11 as a function of distance from the release line. Also shown are calculated dosages for all cases where these values exceeded 1 within the first 24 miles after release.

It is apparent in Fig. 11 that there is little agreement between calculated and observed dosages. In all cases, the cloud arrived at the ground much earlier than computed from the measured turbulence data. A quick comparison of Fig. 11 with Oklahoma dosages shown in Fig. 8 suggests that, for several of the Texas trials, much greater turbulence even than observed in Oklahoma would be required to explain the early arrival of the cloud at the ground in Corpus Christi. In addition, the appearance of the downwind dosage plots shows great variability along the sampler line. Sufficient turbulence to produce the observed arrival of the cloud at the ground would, at the same time, have produced sufficient mixing to produce a more homogeneous downwind dosage distribution.

Depths of the turbulence layer for the Texas trials as measured by the aircraft are shown in Table IV:

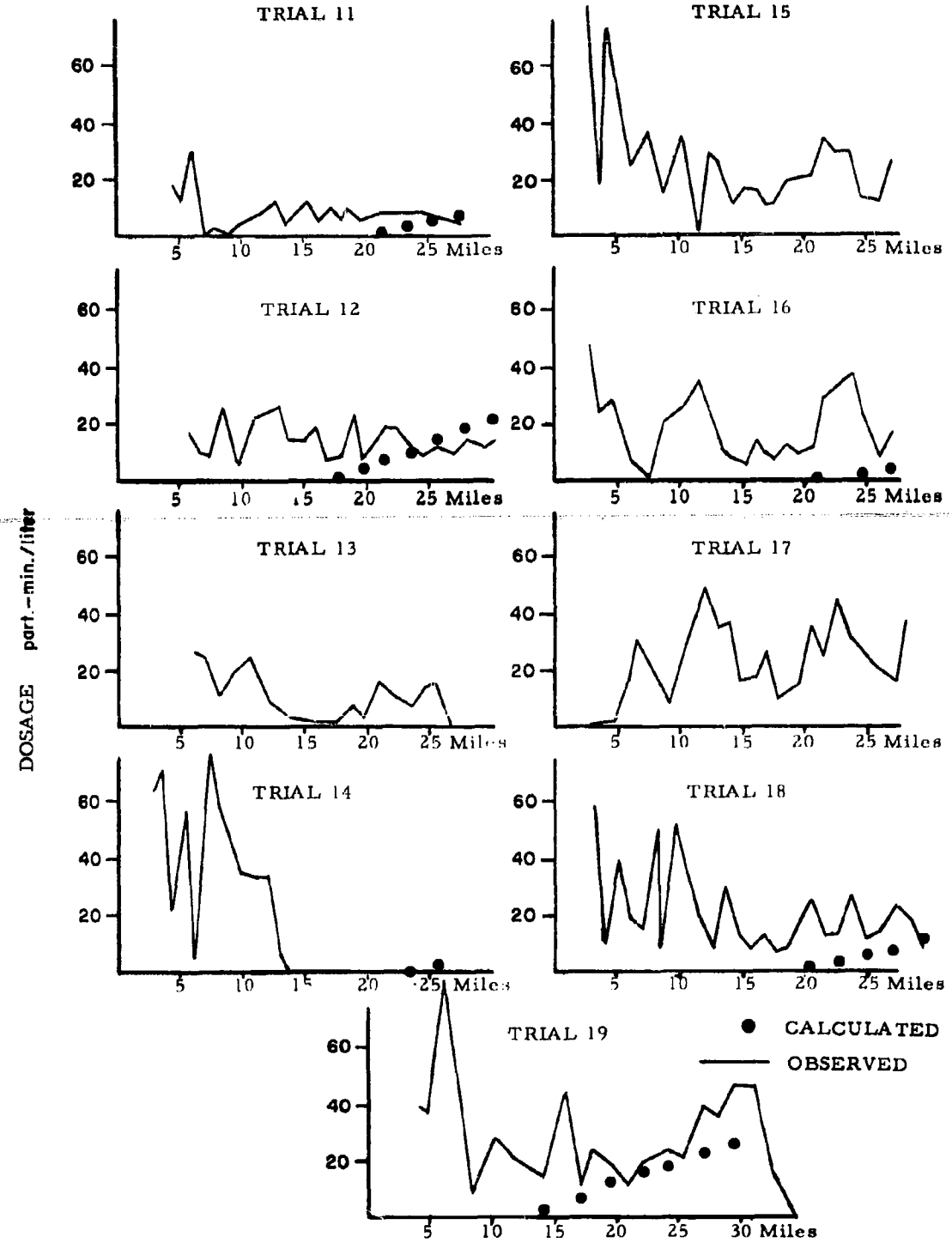

Fig. 11 TEXAS DOSAGES

TABLE IV

DEPTHS OF TURBULENT LAYER

Trial	Layer Depth	Wind Velocity	Box Model Dosage ($\frac{\text{part-min}}{\text{liter}}$)
11	1700 ft	19 mph	13.8
12	700	12	53.1
13	600	16	46.4
14	400	17	65.4
15	300	18	82.6
16	400	14	79.8
17	400	16	69.6
18	600	15	49.6
19	600	15	49.6

Trial 11 was conducted during the afternoon and shows a much greater depth of turbulence; the balance of the trials were carried out during the night and showed turbulent depths of 300 - 700 feet.

Box model dosages computed from measurements of turbulent layer depths and wind speed are generally larger than observed dosages at large distances downwind from the release. This indicates incomplete vertical mixing throughout the turbulent layer and an inhomogeneous vertical cloud distribution.

Since measured turbulent mixing is not of sufficient intensity to explain the ground dosages at Corpus Christi, there must exist an organized flow downward from the release height toward the ground which displaces the center of the cloud downward to where turbulent mixing can transfer a portion of the cloud to actual surface levels. The most reasonable type of organized flow in the Corpus Christi region appears to be helical vortex patterns oriented along the mean wind. These have been observed frequently over warm water ocean area (5). Woodcock has found evidence of this type of motion from observations of bird soaring characteristics within an intermediate range of wind speeds and with water temperatures exceeding air temperatures by 2 - 3°C or more. Under these surface heating conditions, widespread, uniform convection occurs which takes the helical vortex form rather than the more localized, more intense convection patterns commonly observed over land. Pack (6) has shown an interesting observation of this type of motion in which two tetroons, released simultaneously, were caught up in adjacent vortices and executed full helical cycles in opposite directions. Hallanger, et al. (7) have suggested this type of motion as an explanation of certain peculiarities appearing in sampling data from diffusion tests at Camp Cook, California, in 1955-56. In Hallanger's case the widespread lifting was realized mechanically by an onshore wind passing over seashore cliffs.

From the existing observations, this type of flow pattern requires, 1) widespread, uniform lifting of the air in the surface layers, 2) near neutral temperature lapse rates, 3) a more stable layer at, perhaps, 1500 feet to deflect the upward motion toward the crosswind direction, and 4) a moderate wind velocity to organize the motion longitudinally into a helical pattern. It would appear that these conditions are most frequently met over subtropical ocean areas with warm water surface temperatures. These conditions prevail generally in the Corpus Christi area.

The particle cloud during the Texas trials arrived at the ground so rapidly that only one trial (Trial 17) showed near zero dosage on the first sampler (3 miles from release). The release during this trial was made at 1000 feet. In all other trials, substantial dosage was received at the first downwind station. This implies an organized downward flow of about 50 - 100 ft/min during the travel period from the release location.

Small, organized flows of this magnitude are difficult to observe without unusual preparations and techniques. As a consequence, no direct measurements or observations of this flow pattern were obtained during the Texas trials. The conditions for the generation of helical patterns were generally present, however, and it is assumed that this type of flow is the most reasonable analysis of the discrepancies between observed and calculated dosages.

C. Washington

1. Terrain Description

An elevation contour map of the Washington site is shown in Fig. 12. Alternate sampler lines extended north from Colfax to Rosalia and northeast from Colfax to Tekoa. With the exception of the unsuccessful Trial 20, wind directions generally from the southwest dictated the use of the Tekoa sampling line.

The terrain consists principally of wind-generated, sand hills of slightly greater height and more closely spaced than the rolling terrain of the Oklahoma site. Little vegetation is present in the area. In isolated locations, higher buttes rise to about 1200 feet above the sampling line. Roughness of the area is somewhat greater than the Oklahoma or Dallas sites.

2. Meteorological Environment

All trials were conducted in south to southwesterly wind flow conditions. With the exception of Trial 20 no fronts influenced the area during the trials.

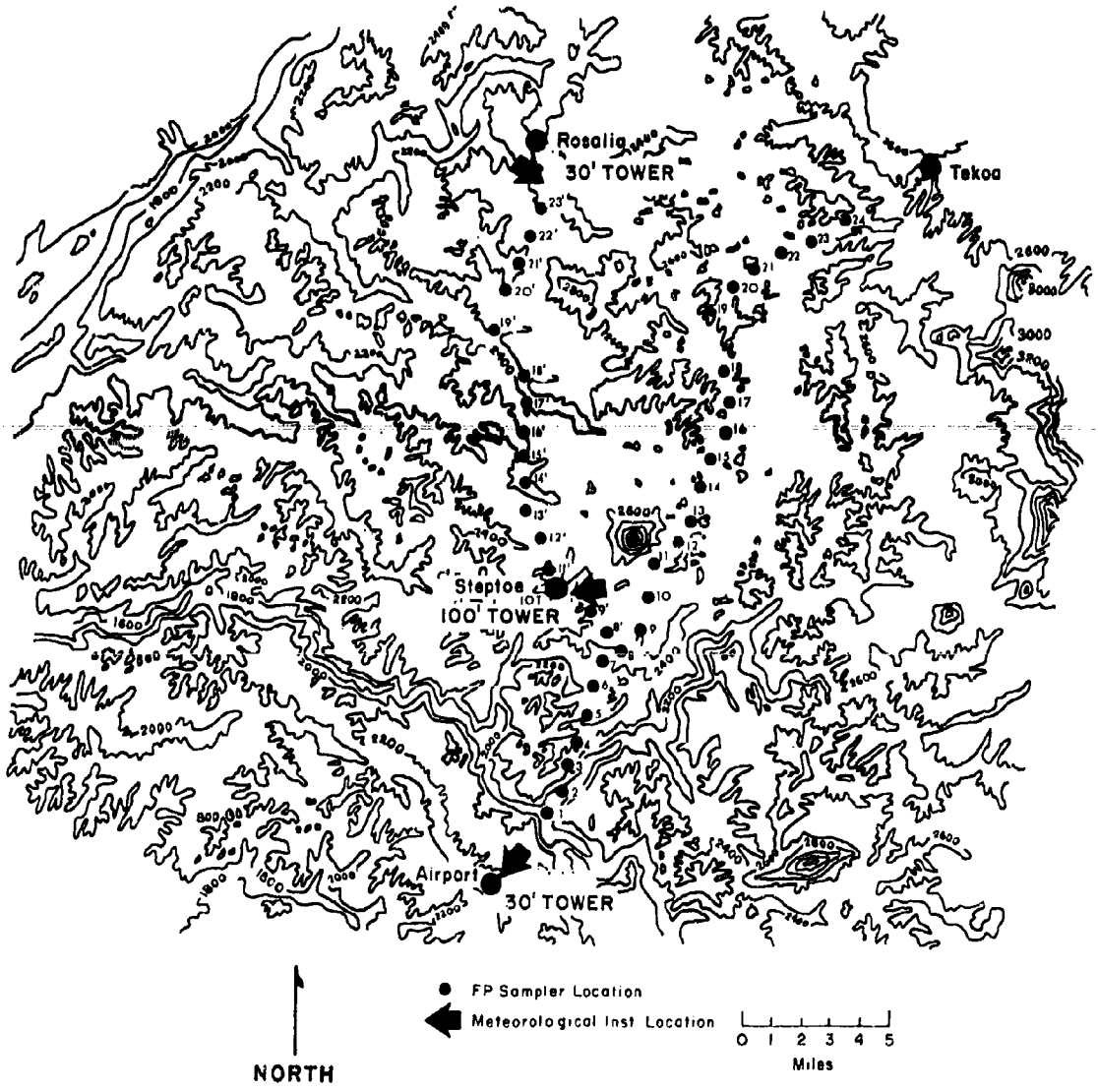

WASHINGTON TEST SITE

Fig. 12

The typical diurnal changes in wind velocity profile are shown in Fig. 13. This figure was drawn from a composite of all pibals taken near the hours shown. Nocturnal increases in winds aloft typical of low level wind jet conditions are clearly seen. Substantial decreases in turbulent mixing from afternoon to evening are responsible for the wind accelerations and high velocities observed during the middle of the night. Peak velocities occur at about 1000 feet and little turbulence would be expected above these levels in the typical nocturnal conditions. Directional wind shears were quite large during the nighttime regime, usually amounting to about 50° (wind veers aloft) in the lowest 2000 feet. Directional shear of this magnitude can only occur under restricted vertical mixing conditions and nocturnal effective turbulence values should be low.

Depths of the turbulent layer, as measured in the aircraft, are shown in Table V together with time of day and observed turbulence values (σ_5) at the standard release height of 1200 feet above most of the sampling line.

TABLE V

DEPTHS OF TURBULENT LAYER

Trial	Local Time	Depth Turbulent Layer	Observed Turbulence at Release Height
21	1452 PST	more than 2000 feet	.84 DEG.
22	1807	2000 feet	1.25
23	2219	1700 feet	.11
24	0136	1700 feet but lower in places	.27
25	1816	more than 2000 feet	1.18
26	1453	more than 2000 feet	.99
27	1805	less than 1000 feet	.20
28	2218	less than 1000 feet	.12

It is to be noted in Table V that afternoon and early evening turbulence at release height is much greater than conditions during the night. In addition, depth of the turbulent layer decreases during the nighttime situations.

Considerable difficulty was found in obtaining sufficient wind velocities at the Washington site for conducting the trials. Three to four weeks were required to accomplish the nine tests involved. Typical wind velocities along the sampler line were extremely light at night. Only occasionally was there sufficient ambient pressure gradient to develop the wind jet conditions shown in Fig. 13 which can lead to momentum transfer downward to the surface layers. Under the conditions of marked radiational cooling typical of the nighttime situation, sufficient temperature stability usually developed to

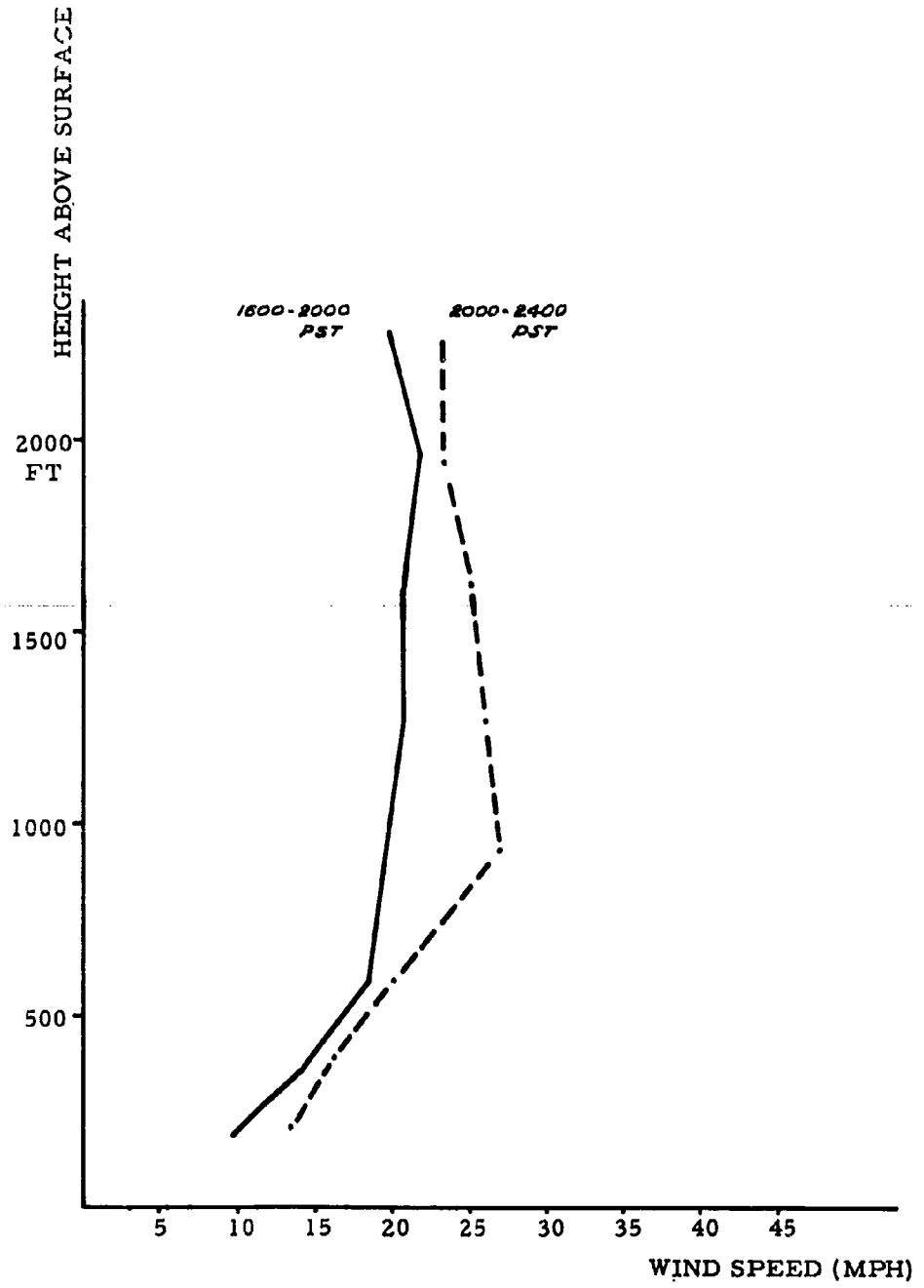

AVERAGE WIND PROFILE - WASHINGTON

Fig. 13

overcome the turbulence-generating effects of the wind shear except under the most pronounced wind jet conditions. Fig. 13 is therefore more typical of extreme nocturnal changes in wind rather than the normal regime.

3. Estimation of Effective Turbulence

Table VI shows effective turbulence values estimated by the three techniques mentioned previously:

TABLE VI

EFFECTIVE TURBULENCE - WASHINGTON

Trial	Stability Factor ($\Delta\theta/u^2$)	100-Foot Turbulence	Release Height Turbulence
21	1.8 DEG.	.5 DEG.	2.3 DEG.
22	1.1	1.35	3.0
23	.7	.5	.55
24	1.1	.5	1.15
25	.6	.4	2.9
26	---*	.65	2.55
27	.4	.5	.95
28	.3	.4	.50

*$\Delta\theta$negative.

Comparison of the various columns in Table VI indicates that effective turbulence values estimated from the aircraft are larger than obtained from any other source. Stability factor and 100-foot turbulence values are in reasonable agreement with each other.

Large aircraft-obtained values are all afternoon or early evening releases when turbulence extended to greater heights. From this standpoint the variations in effective turbulence obtained from the aircraft values appear to be more plausible than those obtained from low level observations. It seems likely that local terrain influences have affected these low level effective turbulence estimates and, in line with previous decisions, the aircraft-obtained effective turbulence has been used in the following section to compute ground dosages.

4. Analysis of Results

Minimum safe flying altitudes at night over the Washington site turned out to be about 1200 feet above most of the sampling line. This altitude corresponded closely to the tops of the isolated buttes in the

area. During the night this restriction meant that releases were made near the peak values of the wind jet where turbulence was slight. As shown previously, turbulence extended well above this altitude during the afternoon and early evening.

Fig. 14 shows observed dosages received during the various Washington trials. Also shown are computed dosage values using aircraft-obtained effective turbulence estimates whenever this computed dosage exceeded 1. Trials 21 and 26 were carried out in the afternoon. On these trials the cloud arrived at the ground earlier and in greater quantity than predicted by the aircraft turbulence even though the aircraft-obtained values were larger than found by any other method. It seems probable that, for these afternoon trials, the aircraft measured turbulence (σ_B) is only a small portion of the existing turbulent energy. Under these convective conditions considerable turbulent energy must exist at much lower frequencies. This energy, not measured by the aircraft and not present in Dallas and Oklahoma, contributes to more rapid downward spreading of the cloud than computed from the σ_B value.

The remainder of the trials in Washington show only small observed ground dosages and small computed dosages as a result of the small existing turbulence levels.

In order to obtain information on dosage distribution around an isolated hill, Steptoe Butte (3 miles NE of Steptoe in Fig. 12) was instrumented with rotorod samplers along a road which winds from the valley floor to the top of the butte. A map of the rotorod locations and elevations is shown in Fig. 15 under the slight simplification of depicting the butte as being circular.

Table VII shows dosage received at the various samplers on Steptoe Butte for each of the trials:

TABLE VII

STEPTOE BUTTE DOSAGES ($\frac{\text{part-min}}{\text{liter}}$)

Sampler	A	B	C	D	E	F	G	H
Trial 21	4.1	1.9	.8	2.0	1.6	3.2	.4	.9
22	2.4	10.4	8.9	9.0	11.8	14.6	13.6	14.1
23	.2	3.5	1.5	.6	3.7	1.4	3.9	2.1
24	.2	6.5	1.9	1.6	11.7	5.4	9.8	10.1
25	.3	.2	1.2	.1	0	.2	.6	.5
26	7.6	4.1	7.0	13.6	9.7	14.6	13.1	2.9
27	0	0	0	0	0	0	.3	0
28	.1	0	0	0	.1	.1	0	0
Average	1.9	3.3	2.6	3.4	4.8	4.4	5.2	3.8

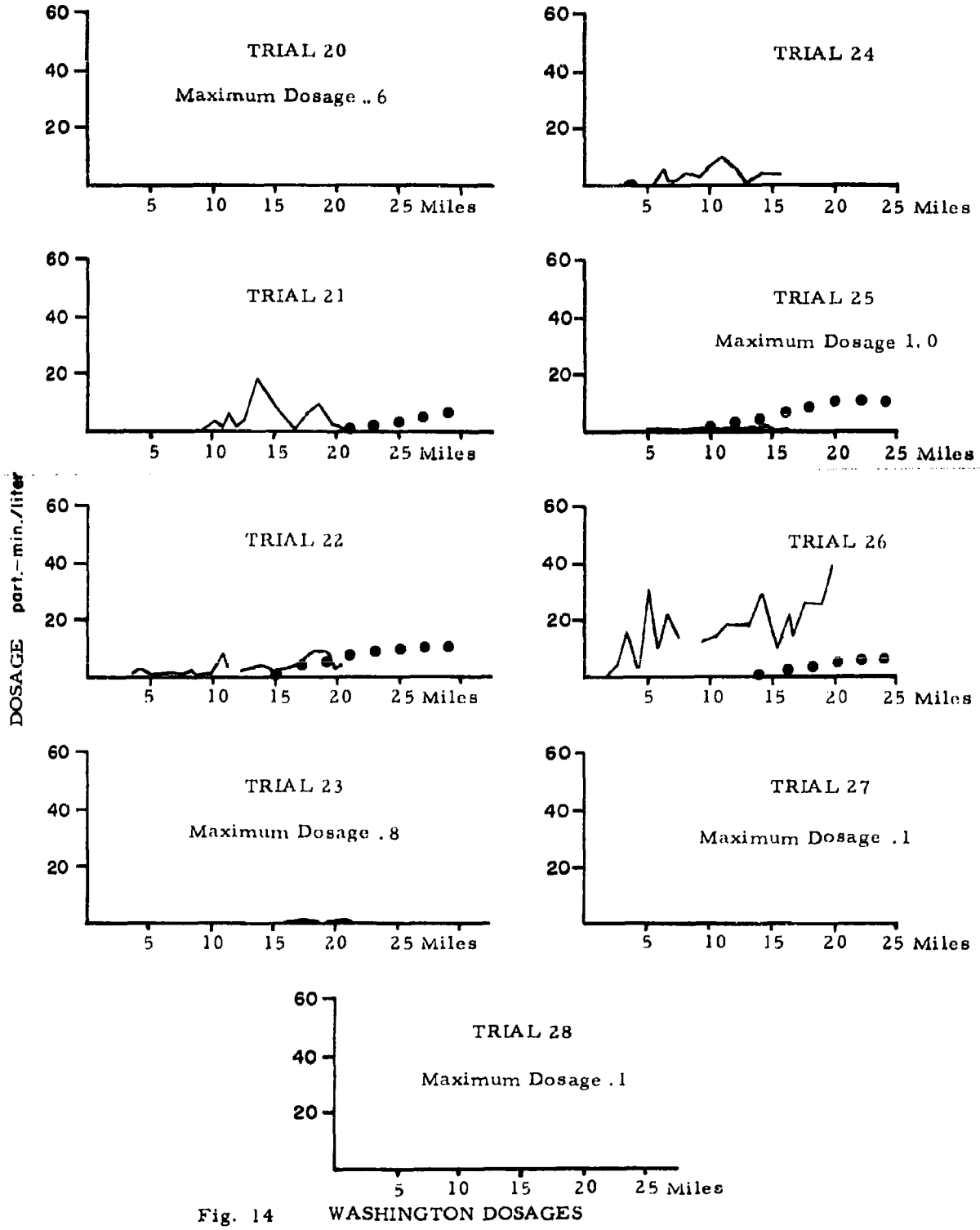

Fig. 14 WASHINGTON DOSAGES

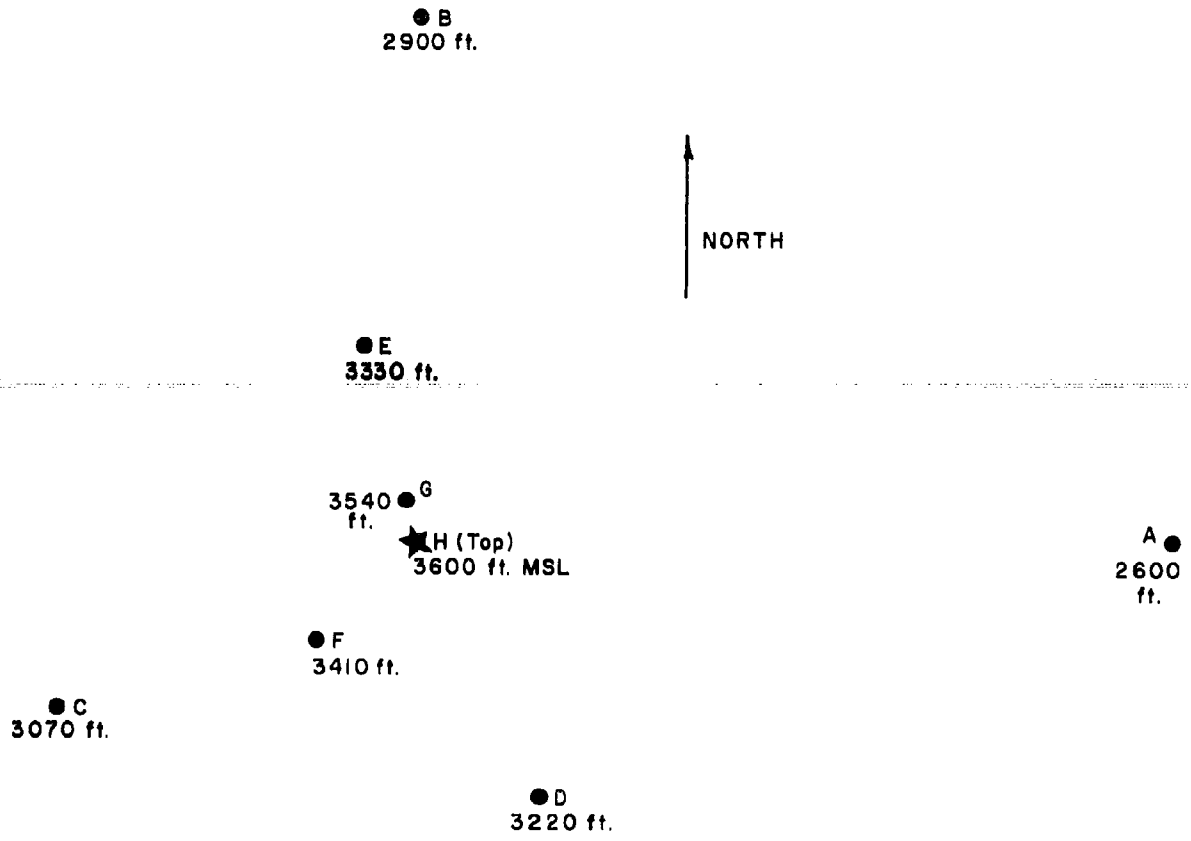

STEPTOE BUTTE SAMPLERS

Fig. 15

Average dosage values in Table VII show a general increase in dosage with height as would be expected under the trial conditions when dosage values along the sampler line were small. A slightly smaller dosage value is shown at the top of the butte, however. The principal feature of the table is the tendency for increased dosage on the lee slope. B dosages were greater than C, E greater than F, and G greater than H in spite of higher elevations for the C, F, and H positions. This lee slope effect is shown more clearly in the Nevada trials and will be discussed in a later section.

Trials 25, 27, and 28 are unusual in showing very low dosage values at all rotorod locations, including the top of the butte. Since the releases were generally made at the same elevation as the top of the butte and only 7 - 11 miles upwind, there is little chance that the cloud failed to pass over the butte. The only reasonable explanation for these low dosages is that the airflow over the butte was deflected upward and the center of the cloud was actually higher than release height as it passed over the butte. Under the stable, low turbulent regime present during these trials, the vertical growth of the cloud was apparently not sufficient to reach the top of the butte in substantial quantity. This type of deflection of the cloud center is also discussed in greater detail in the Nevada trials.

D. Nevada

1. Terrain Description

An elevation contour map of the Nevada site is shown in Fig. 16. An east-west ridge extends across the sampler line in the vicinity of Goldfield. The sampler line runs from an elevation of 5000 feet on the north slope to near 6000 feet on the crest of the ridge to 5000 feet on the south slope. The 100-foot tower was located near the crest of the ridge and the 30-foot towers were placed about 5 miles down the north and south slopes. FP releases were made along an east-west line through West Lake and Mud Lake.

To the west of Goldfield the top of the ridge rises toward an 8000-foot peak which has exerted an influence on the trial results and will be mentioned in the following sections.

A pronounced feature of the ridge is the gradual slope on the north and south sides. On the north the 1000-foot rise is accomplished in 12 - 15 miles. To the south the drop to 5000 feet occurs in about 10 miles.

2. Meteorological Environment

During the late afternoon and night on many days a steady north to northwest wind flow occurs in the Tonopah area and passes easily over the Goldfield ridge without appreciable deflection. Depth of the flow is

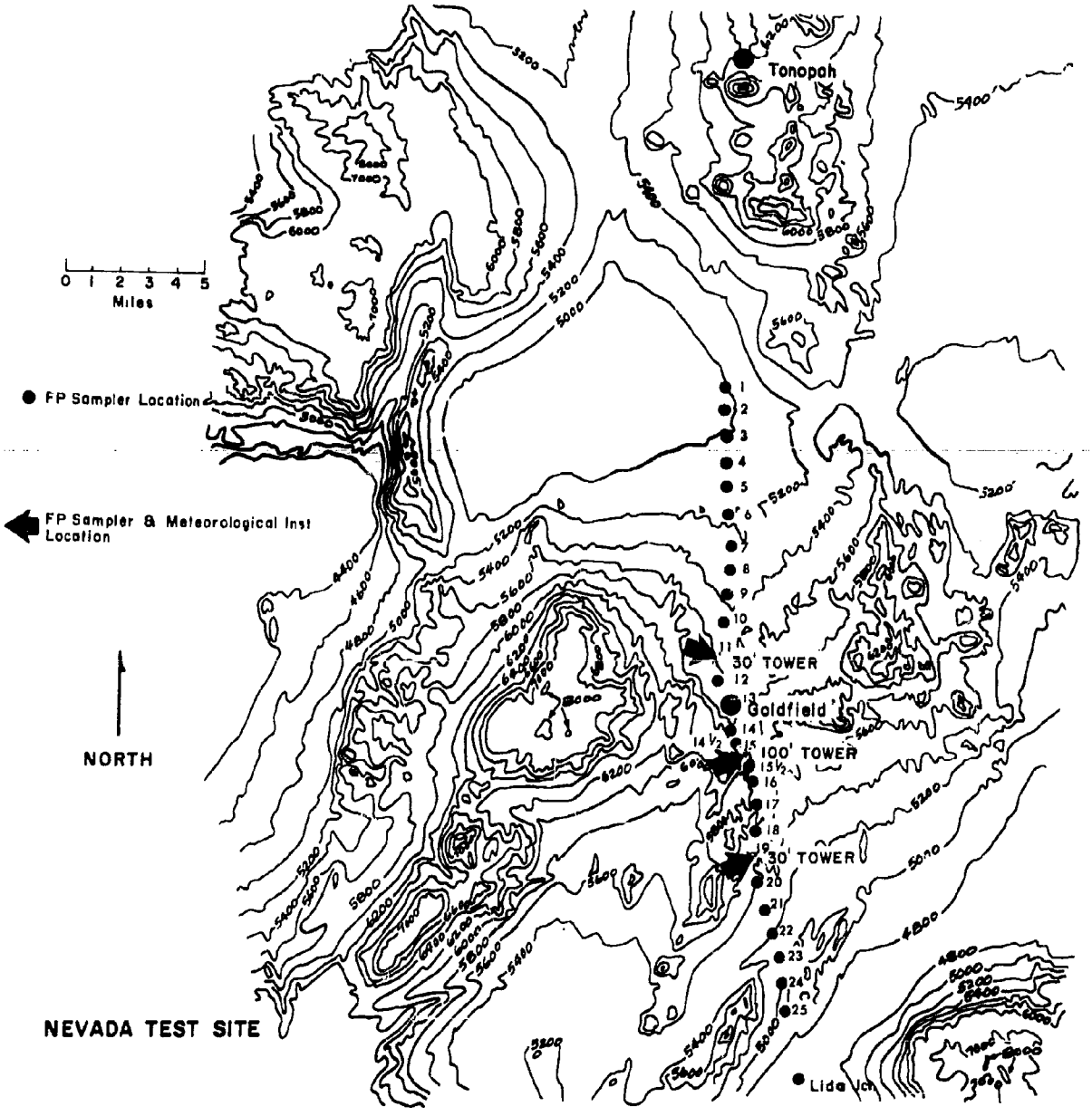
Tonopah
0 1 2 3 4 5
Miles
FP Sampler Location
FP Sampler & Meteorological Inst Location
NORTH
30' TOWER
Goldfield
100' TOWER
30' TOWER
NEVADA TEST SITE

Fig. 16

around 2000 feet. This flow occurs most nights in spite of pressure gradient winds that, during the trial period, were generally directed from the east or southeast. Above 7000 feet MSL strong directional wind shears are present with the wind ultimately becoming southeasterly at higher levels. Below 7000 feet, however, the wind blows steadily from the north or northwest.

This northerly flow is a frequently observed but poorly understood phenomenon at a number of locations along the east side of the Sierra Nevada range. A few suggestions have been made that it represents a massive afternoon and evening drainage from the high Sierra Nevada mountains immediately to the west. As far as is known, it has not yet been adequately documented or described.

The typical nocturnal change in wind velocity at the Nevada site is shown in Fig. 17 which was constructed from all available pibal readings made within the hours shown. During the evening, as the surface layers cool and the temperature lapse rate becomes more stable, the air cannot pass over the ridge as readily as during the afternoon and a general increase in velocity occurs as the air tries to pass through a relatively narrow space over the ridge top. Coupled with this effect is the customary decrease in vertical mixing from afternoon to evening which permits accelerations aloft in the nature of the low level wind jet. Fig. 17 wind profiles appear to result from these two factors.

Radiational cooling effects at night are substantial under the high elevation, dry, desert conditions of the Nevada site. Drainage down the northern (windward) slope and down the southern (leeward) slope results from this radiational cooling. On the northern slope, at the 30-foot tower location, the sequence of wind directions during the night is northerly, west-southwest, and finally, southerly. The west-southwest wind during the early evening apparently occurs when drainage air from the 8000-foot peak immediately west of Goldfield dominates the flow on the northern slope. Later, drainage from the Goldfield ridge itself becomes more important and the wind at the 30-foot northern tower may turn to southerly. On the two nights of the trial period with rather complete wind coverage the change to southerly wind at the north tower occurred around 2300-2400 PST. On the southern slope the drainage flow and the customary lee slope flow are in the same direction and are difficult to separate.

Depths of the turbulent layer over Tonopah airport during the Nevada trials are shown in Table VIII:

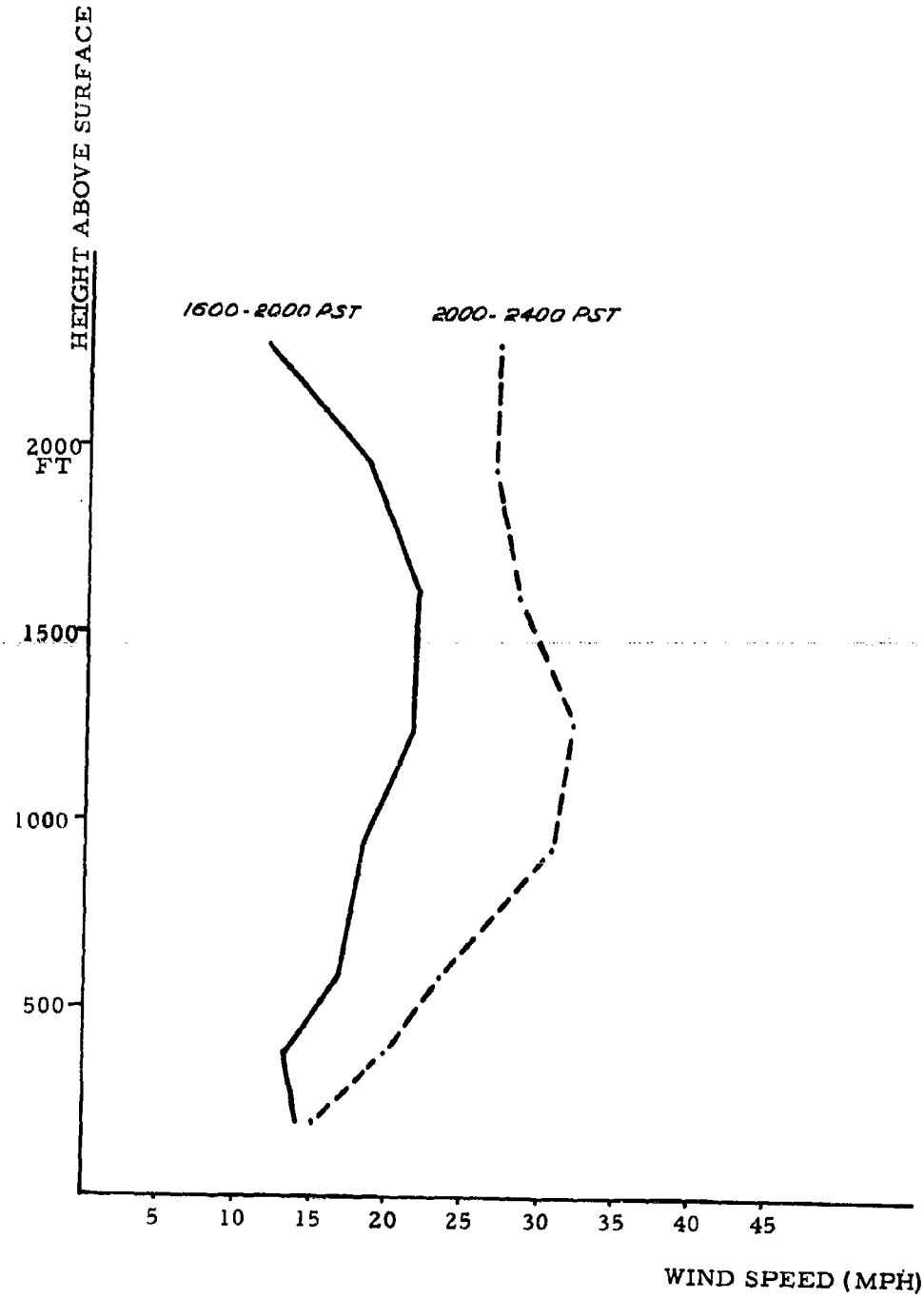

AVERAGE WIND PROFILE - NEVADA

Fig. 17

TABLE VIII

DEPTHS OF TURBULENT LAYER - NEVADA

Trial	Release Time	Layer Depth	σ_5 at Release Height
29	1555 PST	more than 2500 feet	.79 DEG.
30	1918	more than 2500 but lower elsewhere	.14
31	1908	1500	.37
32	2202	600	.58
33	0202	about 2000	1.42
35	1903	more than 2500	.89
36	2154	more than 2500	.85

Trials 29 and 30 were carried out on the same night and show a decrease in turbulent characteristics during the early evening. Trials 31, 32, and 33 were on the same night and show generally low turbulence in the early evening but after midnight, the northwesterly flow decreased in velocity and the observed turbulence level (σ_5) increased. Trials 35 and 36 were conducted on the same night and both show moderate turbulence levels during the early evening.

Comparison of Table VIII with similar data for Washington shows generally similar turbulence levels at release height and considerably more turbulence than was present at release height in Oklahoma or Corpus Christi.

3. Estimation of Effective Turbulence

The use of an effective turbulence value in an area such as the Nevada site is rather meaningless when the terrain rises 1000 feet downwind of the release line. In the first place, the estimated turbulence value changes markedly downwind as the air flows over the ridge. In addition, it has not been possible, as yet, to compute expected dosage values under these conditions of changing terrain and changing turbulence levels. For the sake of completeness, however, effective turbulence values are shown in Table IX as calculated by the various methods described previously:

TABLE IX

EFFECTIVE TURBULENCE VALUES - NEVADA

Trial	Stability Factor ($\Delta\theta/\bar{u}^2$)	100-Foot Turbulence	Release Height Turbulence
29	---*	2.5 DEG.	2.25 DEG.
30	3.1 DEG.	1.5	.70
31	2.9	1.9	1.4
32	1.0	.85	1.85
33	.2	1.15	3.3
35	4.1	1.9	2.4
36	3.0	1.75	2.35

*$\Delta\theta$ negative

In the above table, turbulence at release height was measured about 10 - 15 miles upwind of the ridge while the stability factor and 100-foot turbulence estimates are made from measurements made at the ridge location. In the first case, the release height is about 1300-feet above the terrain at the beginning of the sampler line and the effective turbulence value applies to this entire layer. In the case of the measurements made at the ridge, the effective turbulence value applied to the 400-foot depth from the ridge top to the level of the release. It is clear that all of these values are not comparable and the concept of an effective turbulence value in this case is not clear.

4. Analysis of Results

All releases were made upwind of the ridge at an altitude of about 400 feet above the ridge top. As in Washington, this elevation was primarily dictated by safe night flying restrictions.

Observed ground dosages for the Nevada trials are shown in Fig. 18. Computed dosages using the aircraft-obtained effective turbulence values and assuming the non-existence of the ridge are also shown for those cases where the computed values exceeded 1. The computed dosages essentially show the ground dosages which might be expected from the existing turbulence values at a release height of 1300 feet over flat terrain. In general, the presence of the ridge clearly caused larger ground dosages than would have occurred over flat terrain but it is not possible to carry the computations further due to the present inability to handle inhomogeneous downwind turbulence and terrain conditions.

Trial 29 was the only one carried out during the afternoon at the Nevada site. The cloud clearly came down to the ground rapidly at a

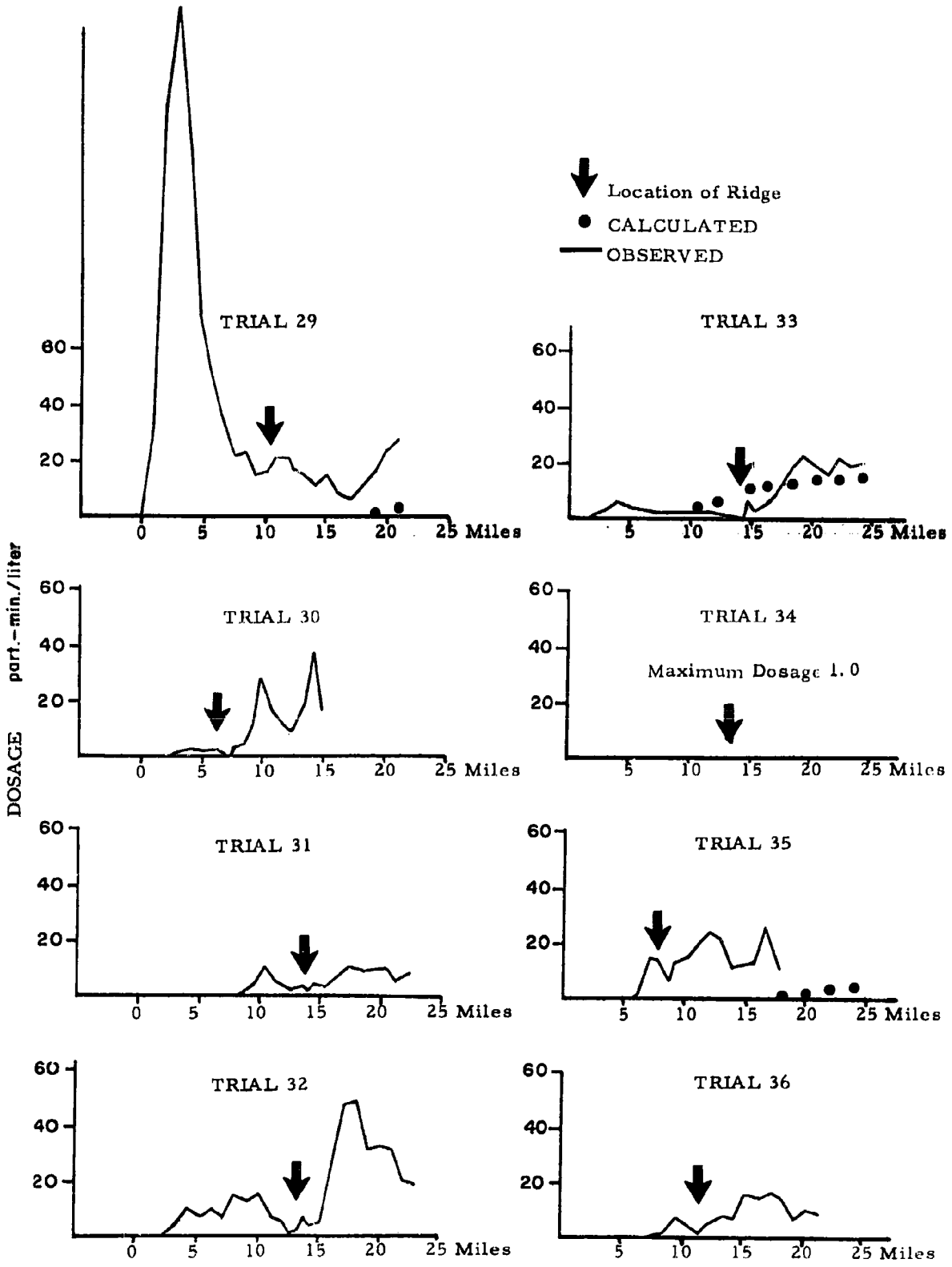

Fig. 18 NEVADA DOSAGES

rate of about 100 - 200 ft/min. As in the Corpus Christi trials, there was insufficient turbulence to produce this rapid downward travel and, also in common with the Texas trials, the large peak value indicates a lack of extensive vertical mixing, i. e., the cloud center must have been displaced rapidly downward toward the ground. Two causes of this flow suggest themselves; a larger convective eddy or downflow in the lee of the ridges near and west of Tonopah. There is insufficient information to carry the subject further but the large dosage could not be the result of the usual turbulent mixing processes.

Following arrival of the cloud in quantity at the ground in Trial 29, a substantial part of the cloud entered the turbulent boundary layer and passed along the entire sampling line with nearly constant dosages.

For the balance of the trials (with the exception of the unsuccessful Trial 34) dosage on the lee slope of the ridge exceeded that observed on the windward slope. Largest dosages on the windward slope occurred in Trial 32, with minor amounts in Trials 31 and 33. During the early portion of the night (Trials 31 and 32) the wind direction at the northern 30-foot tower was from the WNW to WSW as a result of drainage from the 8000-foot peak west of Goldfield. Between Trials 32 and 33 the wind at the 30-foot tower shifted to south as air from the Goldfield area began to drain downward to the north.

On the basis of temperature and wind data on the northern slope, the following sequence of events apparently occurred during the night:

Trial 31 (1908 PST) - Wind flow on the northern slope was westerly but no substantial drop in temperature had yet occurred. A small amount of cloud material entered the sampling line from the side as the result of distortion of the flow by the 8000-foot peak to the west of the line. However, a true drainage wind had not yet occurred.

Trial 32 (2202 PST) - The temperature dropped appreciably at the north tower and the wind continued from the W to WSW. Drainage air reached the sampler line from the side, having originated on the slope of the 8000-foot peak to the west. With the actual release height around 1600 feet below the top of the peak, cloud material easily entered the drainage flow and moved eastward toward the sampling line.

Trial 33 (0202 PST) - The wind at the north tower shifted to south as drainage flow from the Goldfield slope reached the tower. A further temperature drop occurred. Dosages at this point on the slope were much lower than in the previous test and it would appear that cloud material did not enter the drainage flow in the Goldfield region. This is further substantiated by very low dosages at the top of the ridge. Small dosages near the beginning of the sampler line probably resulted from a westerly-type drainage wind although no wind data are available for this location.

During Trials 30, 35, and 36, the wind direction at the 30-foot tower remained northerly, the drainage flow did not begin until later in the night and no appreciable dosages appeared on the windward side.

Table X shows the dosages received at the top of the ridge (top of the 100-foot tower) for each of the trials:

TABLE X

RIDGE CREST DOSAGES - NEVADA

Trial	Dosages $\left(\frac{\text{part-min}}{\text{liter}}\right)$	Local Time	Date
29	20.7	1555 PST	10/31
30	1.3	1918	10/31
31	4.6	1908	11/1
32	1.9	2202	11/1
33	1.0	0202	11/2
35	11.2	1903	11/5
36	5.3	2154	11/5

The general trend in Table X is for dosages at the top of the ridge to decrease during the night as the vertical temperature structure becomes more stable. Under these circumstances it becomes more difficult as the night progresses to inject cloud material into the drainage flow on the windward slope if the release is made above the ridge top.

Along the lee slope, the principal problem in analyzing the trials arises from the need for understanding the flow pattern in the lee of the ridge. One technique for accomplishing this is shown in Figs. 19 and 20. Potential temperature surfaces in these figures have been constructed from vertical temperature soundings made by the aircraft runs over the ridge at 1000 and 2000 feet above the ridge. Additional data come from potential temperature and wind data at the 30-foot level on each of the three towers on the slope. During the nighttime stable conditions, at some level above the ridge, the potential temperature surfaces must also be streamflow surfaces. Near the slope of the ridge, local radiational cooling leads to non-isentropic flow and the potential temperature surfaces no longer correspond to flow patterns. In Figs. 19 and 20, streamflow patterns are drawn which fit the potential temperature surfaces aloft but deviate to fit tower winds and logical flow patterns near the ridge slope.

In Fig. 19, Trial 29 is typical of convective type afternoon heating regimes. Through a considerable layer above the slope, particularly on the upwind side, potential temperatures are nearly constant with

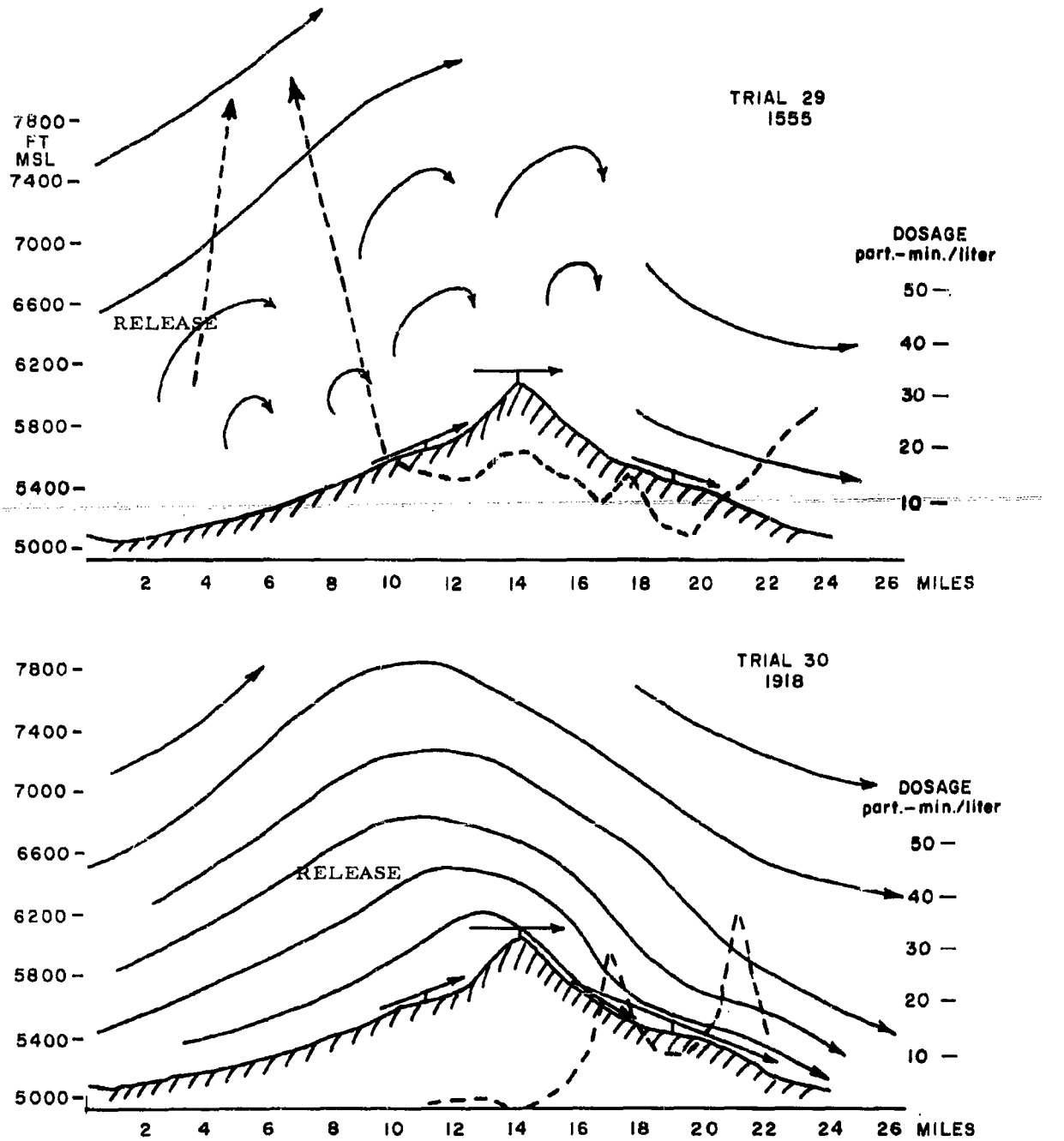

SCHEMATIC FLOW PATTERNS OVER NEVADA RIDGE

Fig. 19

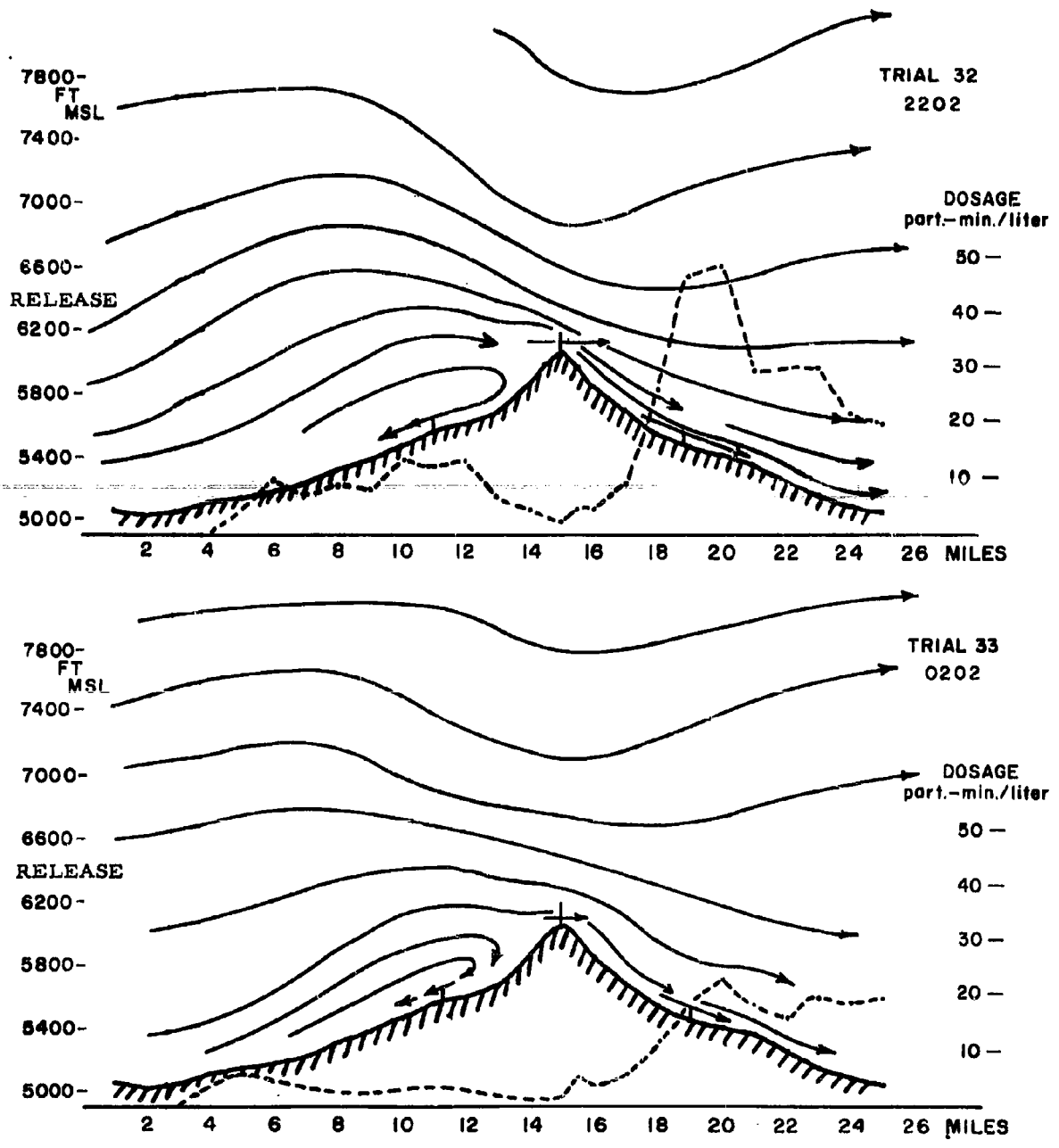

SCHEMATIC FLOW PATTERNS OVER NEVADA RIDGE

Fig. 20

height, indicating considerable vertical mixing. By 1918 when Trial 30 was carried out, considerable temperature stratification had occurred and the flow pattern over the ridge indicates a peak air flow displaced upwind of the ridge top. This obviously carried the center of the cloud upward, protecting the windward slope and, to a large extent, the ridge top from observed dosages. Considerable downward flow occurs over and in the lee of the ridge and the cloud material is brought downward close enough to the lee slope for substantial quantities to reach the ground.

Similar patterns are shown in Fig. 20 for Trials 32 and 33 although the peak of the air flow is displaced even farther upwind of the ridge top. The principal difference between Trials 32 and 33 is the lower wind velocity in Trial 33. Wind at release height decreased from 17 mph for Trial 32 to 11 mph in Trial 33. The resulting change in flow pattern was to make the air flow peak somewhat less pronounced and the downslope flow in the lee of the ridge somewhat weaker. The changes in dosage on the lee slope follow this pattern of change in lee slope flow and are shown in Fig. 20.

Wind flows on the slope at each tower location are shown in vector form in Figs. 19 and 20. Attention is called to the strong downslope winds at the south tower, particularly in Trial 32. From a continuity standpoint stronger flow at the south tower than the ridge top requires additional air to be brought to the south slope from higher levels above the ridge to satisfy the requirements for increased air flow near the surface. This also serves to bring additional cloud material downward to the slope.

The type of flow pattern shown for Trials 30, 32, and 33 suggests that it may be very difficult to distribute cloud material on the windward slope of the ridge under stable, nighttime conditions. The indications from the trials are that releases should be made at or even below ridge top in order to have any likelihood of injecting material into the drainage flow on the windward slope. At the same time, the trials show that it is comparatively easy to distribute material on the lee slope from various release heights.

V. DISCUSSION OF RESULTS

A. Terrain Comparisons

Most quantitative studies of terrain characteristics are intended for hydrologic and related purposes and do not adequately describe the roughness features which generate turbulence in the low levels of the atmosphere. From an excellent summary by Carr and Van Lopik (10) of over 60 techniques for quantitative terrain descriptions, only two appear to be applicable to air turbulence problems.

1. Elevation-Relief Ratio

Elevation-Relief ratio (ER) is defined as:

$$ER = \frac{E - L}{R}$$

where E is the average elevation of the area. L is the lowest elevation in the area, and R (the relief) is the difference between the highest and lowest elevation in the area.

The Elevation-Relief ratio may vary from 0 to 1 and primarily measures the relative proportion of land at high and low elevations. Very low numbers signify a generally flat area with isolated peaks. Large numbers (near 1) are associated with a plateau-type terrain cut by narrow valleys.

For the terrains of interest in the present work:

	Elevation-Relief Ratio
Dallas Tower	.71
Oklahoma	.40
Washington	.26
Nevada	.40

The ratio was not calculated for the Corpus Christi area since there is little terrain variation in the region.

The values shown above suggest that Dallas is primarily a plateau-type terrain and Washington tends to feature isolated peaks or ridges. However, in Oklahoma and Nevada the high and low elevation regions are inclined to be more uniformly distributed. Although this is a useful technique for describing the terrain character of an area it has limited applicability for turbulence-generating problems since no measure of the height of the generating elements is included. It is clear, for

example, that a useful system must be able to differentiate between the rolling hills of Oklahoma and the much larger ridge-valley systems of Nevada.

2. Grain and Relief

A second quantitative terrain description makes use of two independent values, grain and relief.

Relief is defined in the same manner as above -- the difference in elevation between the highest and lowest points in the area under consideration. In order to obtain a measure of the grain, an area of 1-mile diameter, for example, is selected and the relief determined. A second circle of 2-mile diameter is then marked off from the same center and the relief again determined. Such values of relief are then plotted as a function of diameter of the area, the relief increasing monotonically with diameter. At some area diameter, further increase in size of area produces only slight increases in relief. This point (area diameter) is termed the grain of the area. It essentially represents the dominant distance between principal terrain features. The accompanying value of relief at this point then represents the size of the terrain features.

In the areas of present interest:

	Grain	Relief
Dallas Tower	20 miles	300 feet
Oklahoma	15	300
Washington	14	1800
Nevada	25	4000

On this basis, the Dallas and Oklahoma areas are seen to be similar in terrain features, Washington and Nevada, however, have much greater relief, and the spacing between terrain features in Nevada is particularly large.

B. Turbulence Comparisons

Vertical profiles of turbulent energy have been plotted in Fig. 21 for the four test areas and compared to profiles observed in the Dallas program. Turbulent energy has been calculated as $(\sigma_5 u)^2$ where σ_5 is the turbulence sigma for 5-second sampling and u is the wind velocity at the same level. Both 100-foot tower data and aircraft data were used to obtain the profiles for Oklahoma, Texas, Washington, and Nevada. These profiles represent the average turbulence levels for all cases for which adequate information was available for computation of the average at all levels.

Attention in Fig. 21 should be devoted to the shapes of the turbulence profiles rather than a comparison of absolute values for the various areas. Absolute magnitudes are primarily a function of wind speed (squared) while the terrain exerts its major influence on the shape of the profile. The principal features of interest in Fig. 21 are the similarities in profile between Dallas and Oklahoma, the very rapid decrease in turbulence with height at Corpus Christi and the relatively uniform turbulence profiles to 2000 ft at Washington and Nevada.

Consideration of the relief values given in the preceding sections suggests the higher relief regions maintain nearly constant turbulent energies to much greater heights. The energy appears to be maintained to a height roughly comparable with the relief height. Grain undoubtedly plays a role in turbulence generation but is likely to be of secondary importance relative to the relief.

The turbulence profiles shown in Fig. 21 are of particular importance when an attempt is made to estimate effective turbulence from release to ground from a single point measurement of the turbulence. Similar profiles of turbulence suggest that estimates of effective turbulence for Oklahoma should be similar to Dallas effective turbulence values if either release height or 100-ft tower data are used to provide the estimate. In the case of Corpus Christi, however, a turbulence reading at release height would lead to an underestimate and a 100-ft tower value an overestimate in effective turbulence if a Dallas profile was assumed. Washington and Nevada effective turbulence values would also be incorrectly estimated through use of the Dallas profile since the turbulent energy aloft is considerably greater than usually occurs with the Dallas type profile.

The form of the turbulence profile consequently determines the method of computing effective turbulence and this technique will need to vary according to terrain. A first approximation for various terrains will be found by maintaining turbulent energy (not sigma) relatively constant with height to a level above ground indicated by the relief of the area.

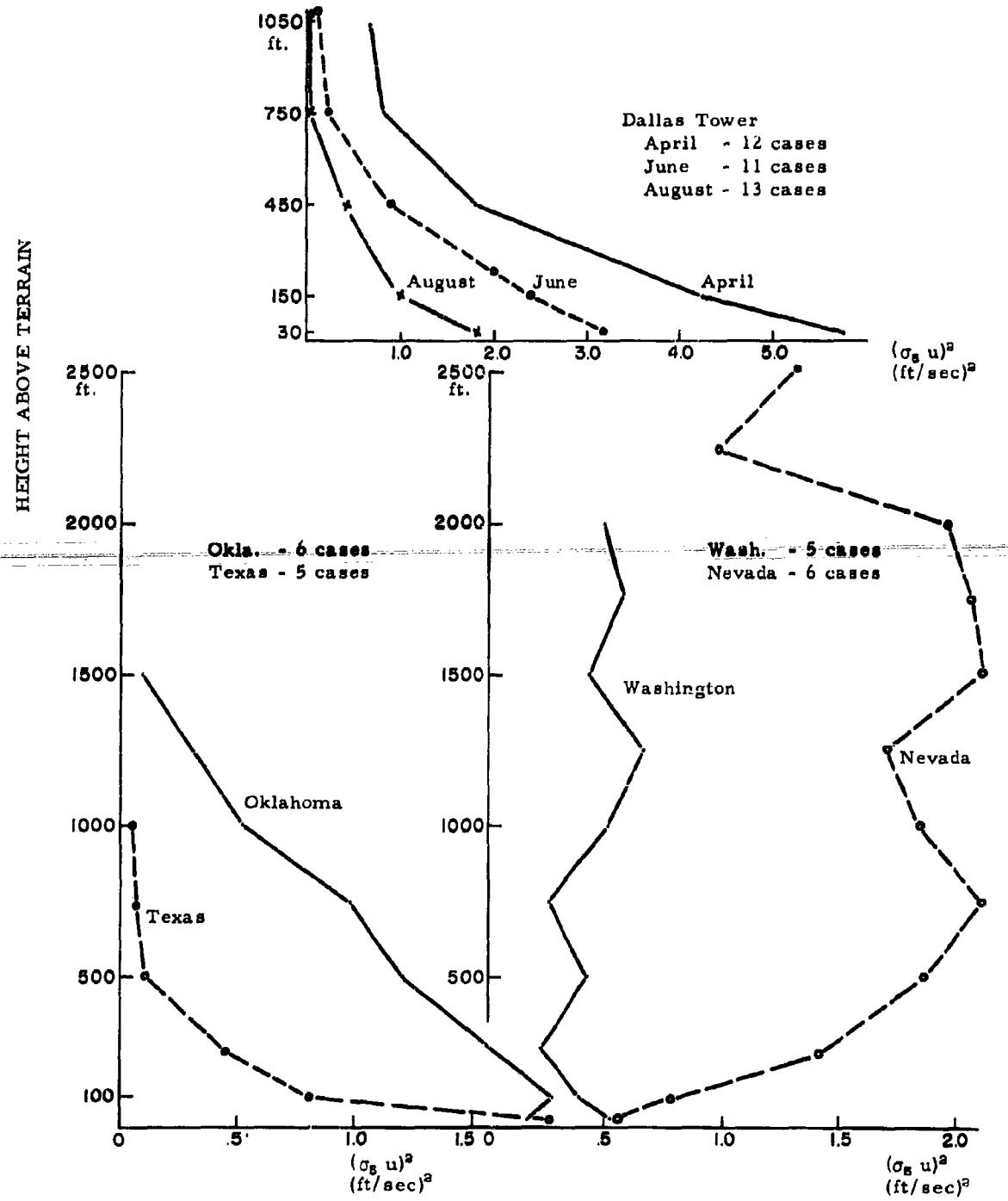

Fig. 21. COMPOSITE TURBULENT ENERGY PROFILES.

Thereafter, for nocturnal turbulence the turbulent energy will usually decrease rather rapidly with height in the manner shown in Fig. 21.

C. Dosage Models

It has been indicated that effective turbulence values for Oklahoma, computed with the aid of the Dallas turbulence profile, give ground dosage values which are in reasonable agreement with observed dosages. Also, in Washington the effective turbulence values would suggest that little FP material would have reached the ground in most cases and little was observed. As a consequence there is no indication that a reasonably computed effective turbulence value would not prove suitable in the Washington area.

For Corpus Christi and Nevada, however, no computed effective turbulence values are able to explain the observed dosages. In both cases, the observed dosages were larger than estimated from the effective turbulence values. This can only be realized by bringing the center of the cloud downward below the height of release. Thus, dosage models for both areas involve primarily the location of the center of the cloud.

In the absence of a meteorological description of the path of the center of the cloud, a measure of the location might be obtained from the sampling data. Maximum dosage is given by the following equation (Ref. 1):

$$D_{max} = .485 \frac{Q}{uH}$$

where Q is source strength, u is average wind velocity, and H is height. If the observed maximum dosage, Q and u, are entered in the above equation, a height H can be computed which might give a measure of the actual height of the cloud.

For the Corpus Christi trials the following data pertain:

	D_{max}	u	$H_{calc.}$	H_{time}	Distance to D_{max}
Trial 11	28.7 $\frac{\text{part-min}}{\text{liter}}$	19 mph	390 ft	500 ft	6.0 miles
12	42.8	12	415	500	4.9
13	26.8	16	500	500	6.1
14	77.0	17	164	500	3.4
15	78.9	18	151	750	2.9
16	47.1	14	324	500	2.9
17	48.3	16	278	1000	12.1
18	57.4	15	248	500	3.3
19	82.5	15	173	500	6.2

$Q = 3.64 \times 10^9$ particles/meter.

In Trials 11 - 13 only slight displacements downward are needed to explain the maximum dosage but, as indicated earlier, there is insufficient turbulence to cause the maximum dosage to occur at 5 - 6 miles. This required turbulence can be estimated from:

$$X_{max} = \frac{H}{3i_e^2}$$

and for Trial 11 becomes 3.7° between 390 ft and the ground. Since the 100-ft tower value is 3.4° and the turbulence decreases rapidly aloft the value of 3.7° is not reasonable for the conditions of the trial.

Similarly, for Trial 15 the required effective turbulence value, i_e, would be 3.3° from 750 ft to the ground, compared to a measured value of 3.3° at 100 ft. Other trials show similar results and it appears that a simple displacement of the cloud center downward will not satisfy both the observed maximum dosage and the maximum dosage distance.

Additional information of interest comes from the computed box model dosages shown earlier in Table IV. With the exception of Trial 11 these figures show that a thoroughly mixed cloud throughout the turbulent layer would produce a larger dosage than observed at the ground. This indicates that most of the cloud has passed aloft over the sampler line and that only sporadic intrusions, presumably associated with the helical eddies, bring sufficient material into the low level turbulent layer to mix downward to the ground. This will be a difficult problem to model and additional data will be required.

Similarly for the Nevada trials the primary problem in modeling the dosage involves a description of the trajectory of the center of the cloud. Flow over ridges may take a variety of forms depending on wind velocities over the ridge, temperature stability, and width of the ridge. On occasions the crest of the flow over the ridge may occur upwind of the ridge as in Figs. 19 and 20 and, at times, the flow in the lee of the wave crest may parallel the lee slopes (Trial 30 - Fig. 19). As the velocity decreases aloft the wave crest over the ridge moves toward the ridge top (Fig. 20). In this case, the flow down the lee slope is not as pronounced and more turbulent mixing occurs in the lee of the ridge. Under other conditions of stability and ridge width the crest of the flow aloft may occur downwind of the ridge and extensive turbulence will be present on the lee slope. Modeling of the dosage over the ridge first requires the establishment of the wave flow pattern aloft both as to position of the wave crest with respect to the ridge and amplitude of the crest.

All of the nocturnal Nevada tests show wave crests upstream of the ridge but by differing amounts, ranging from 3 - 6 miles. Trials 30, 32, 35 and 36 show the greatest amplitude in the wave flow. This is primarily connected with wind flow velocities over the ridge:

Trial	100-ft Wind on Ridge	Maximum Dosage in Lee
30	14.0 mph	27.9 $\frac{\text{part-min}}{\text{liter}}$
31	5.4	10.6
32	9.4	48.5
33	3.2	22.3
35	13.0	23.2
36	11.0	16.0

As indicated above the maximum dosages in the lee of the ridge tend to be larger for those flow patterns with large amplitudes.

Using the same method of investigating maximum dosage values as used above for the Corpus Christi trials:

Trial	D_{max}	u	$H_{calc.}$	Distance to D_{max}*
30	27.9 $\frac{\text{part-min}}{\text{liter}}$	15.0 mph	515 ft	6.1 miles
31	10.6	6.7	2900	10.8
32	48.5	8.5	518	9.8
33	22.3	3.4	2820	8.9
35	23.2	14.3	645	9.7
36	16.0	13.6	985	11.8

*Distance to maximum from wave crest.

These values suggest a dosage model based on a downwind distance along the streamlines, measured from the crest of the wave flow or perhaps from the release point itself. The original release was made 400 ft above the ridge top and the material rose in altitude passing through the crest of the wave and thence the center of the cloud moved downward along the lee slope. Tracing of the streamlines for Trials 30 and 32 (Figs. 19 and 20) will indicate that the streamline passing through the release location also passed some 500 - 600 ft above the position of maximum dosage. An effective turbulence value of about 3° operating on the cloud from the wave crest would result in the location of the maximum observed dosage. In the case of Trials 33 and 35 (light wind cases with poor lee slope flow) it is apparent that the flow down the slope was not sufficiently pronounced to bring the cloud near the ground where substantial turbulent mixing might operate.

It is suggested that the dosage over the ridge may be handled on a model basis only if the flow streamlines are available for tracing the path of the center of the cloud. Thereafter, normal turbulent mixing may be applied to the growth of the cloud downward toward the ground. The streamline flow patterns will fall into a large variety of categories depending on meteorological and terrain conditions. The derived dosage must follow the same type of categories.

VI. CONCLUSIONS

1. Effective turbulence values have been computed by three methods from the data generated during the present program. Under relatively uncomplicated terrain conditions such as the Oklahoma site, these effective turbulence values may be used to estimate ground dosage values providing the turbulence values are representative of the early portions of the cloud travel between release and arrival of the cloud at the ground.

2. Since the cloud from an elevated release spends a large amount of its travel time in the low turbulence regime near release height, turbulence values at release height are most important in estimating ground dosage. Turbulence values measured in the immediate surface layers are frequently subject to local influences and may not reflect the conditions throughout the layer from ground to release height.

3. Terrain conditions need not be very complex before organized flow patterns of a non-turbulent nature are encountered which displace the center of the cloud substantially. Organized coastal flow patterns at Corpus Christi and ridge flows at Nevada contribute more to the determination of ground dosage characteristics than do the observed features of the turbulent mixing.

4. Observed Oklahoma ground dosages corresponded closely to values computed from measured turbulence and the Dallas Tower ground dosage model.

5. In the Corpus Christi trials, an organized flow pattern, probably of a helical vortex form, served to bring the cloud rapidly to the ground in spite of the low ambient turbulence values.

6. Releases in the Washington area were made at such a height that turbulence was generally insufficient at night to bring the cloud to the ground along the sampler line. During two afternoon trials, additional turbulence of a convective nature resulted in small quantities of material reaching the ground.

7. In the Nevada trials, with releases above the height of the Goldfield ridge, substantial quantities of material were brought to the ground on the lee slope of the ridge. The windward slope did not receive large dosages except from the apparent effects of lateral flow across the sampler line.

VII. RECOMMENDATIONS

1. It proved very difficult, during the site selection phase of this program, to select locations with relatively homogeneous turbulence in the downwind direction. The great majority of possible sites and terrain regimes have associated with them small scale flows which displace the center of the cloud in a manner not as readily understood at present as is the turbulent mixing process Additional meteorological work is needed to increase the understanding of these local flow patterns such as mountain-valley flows, flow over ridges, sea-breeze patterns, and helical flows such as may often occur over ocean areas.

2. No dosage model is available for use in conditions of inhomogeneous turbulence in the vertical or downwind directions. From existing data on this program and others, some ideas of the possible variability of these turbulence values have been obtained. The most profitable next step would be to hypothesize various turbulence inhomogeneities of a reasonable character and to compute dosages under these non-uniform conditions by iterative, computer techniques. In this way, effects on dosage of various inhomogeneities in turbulence could be determined and the extent to which these inhomogeneities must be measured can be found. By far the easiest source configuration to use in attempts at calculating the effects of inhomogeneous turbulence is the elevated line source system since the growth rate of the cloud is constant and a function of ($3i^2$) over a considerable distance or time.

3. Measurement of ambient turbulence, air flow patterns, and temperature structure by aircraft methods have progressed further than in any previous program. As additional data are required over varying terrain and in inhomogeneous turbulence conditions, the aircraft will prove to be an increasingly useful tool and should be emphasized in future programs.

VIII. ACKNOWLEDGMENTS

MRI personnel who performed the field tests during this program included M. A. Wolf, J. Gretta, R. Howard, and B. McManus. P. MacCready, Jr., contributed greatly to the program through the development of the turbulence meter and the interpretation of its records.

Assessment of the sampling data was provided by Dugway Proving Ground through contract with Utah State University.

Synoptic weather data in the form of original teletype records were furnished by the Los Angeles office of the U. S. Weather Bureau.

REFERENCES

(1) MacCready, P. B., Jr., et al., 1961: Vertical Diffusion from a Low Altitude Line Source - Dallas Tower Studies, Vol. I and II, Final Report, Contract DA-42-007-CML-504, Meteorology Research, Inc.

(2) Hay, J. S., and F. Pasquill, 1959: Diffusion from a Continuous Source in Relation to the Spectrum and Scale of Turbulence, Advances in Geophysics, 6, New York, Academic Press, 345-365.

(3) Smith, F. B., and J. S. Hay, 1961: The Expansion of Clusters of Particles in the Atmosphere, Quart. J. R. Meteor. Soc., 87, 371, 82-101.

(4) Pasquill, F., 1962: Atmospheric Diffusion, New York, D. Van Nostrand Co.

(5) Woodcock, A. H., 1942: Soaring Over the Open Sea, Scientific Monthly, Sept., 226-232.

(6) Pack, D., 1962: Air Trajectories and Turbulence Statistics from Weather Radar Using Tetroons and Radar Transponders, Mo. Weather Rev., 90, 491-506.

(7) Hallanger, N. L., et al., 1962: Quasi-Stationary Waves Observed in Aerosol Diffusion Trials Conducted in a Coastal Area, J. of Atmos. Sciences, 19, 1, 99-106.

(8) Webster, F. X., 1963: Collection Efficiency of the Rotorod FP Sampler, Tech. Rept. No. 98, Contract DA-42-007-CML-543, Metronics Assoc.

(9) Jones, J. I. P., and F. Pasquill, 1959: An Experimental System for Directly Recording Statistics of the Intensity of Atmospheric Turbulence, Quart. J. R. Meteor. Soc., 85, 225-236.

(10) Carr, D. D., and J. R. Van Lopik, 1962: Terrain Quantification, Final Rept., Contract AF19(628)-481, Texas Instruments, Inc.

APPENDIX A

COMPARISON OF ROTOROD AND FILTER SAMPLERS

Field comparisons of rotorod and filter sampler counts have been made during the Dallas Tower program (Contract 504) and during the present program (Contract 545). Separation of the samplers in the Dallas data was several feet at the base of the tower while separation at the downwind locations was from less than 1/4 mile to about 1/2 mile. In the present program separation of the comparative rotorod and filter samplers did not exceed two feet.

In each program there were 53 pairs of data for which FP counts were observed on at least one sampler. Dallas comparative data have been reported previously (1). The following table shows the comparative data from the present program for the 25 pairs of data for which filter counts exceeded 100. Effective rotorod sampling rate was determined as the product of the ratio of rotorod sampler to filter sampler counts and the filter sampler sampling rate of 6.5 liters/min (100% efficiency).

TEST	FILTER COUNT	ROTOROD COUNT	ROTOROD CT. / FILTER CT.	EFF. ROTO-ROD RATE (liters/min)
1	291	841	2.89	18.8
2	190	700	3.69	24.0
2	144	655	4.62	30.0
3	212	705	3.32	21.6
3	183	1050	5.74	37.3
5	508	2103	4.15	27.0
5	182	1033	5.68	36.9
6	227	1612	7.10	46.2
6	154	634	4.12	26.8
7	173	1640	9.47	61.5
7	275	946	3.44	22.4
7	159	902	5.67	36.9
8	103	465	4.51	29.3
8	178	792	4.45	28.9
8	135	722	5.35	34.8
9	278	643	2.31	15.0
9	113	595	5.27	34.3
12	329	1613	4.90	31.8
14	102	377	3.69	24.0
15	106	912	8.60	55.9
17	212	786	3.71	24.1
18	370	1364	3.69	24.0
19	103	700	6.79	44.1
19	194	643	3.32	21.6
22	116	197	1.70	11.0

Webster (8) has recently published data on the efficiency of the rotorod sampler as a function of average fluorescent particle size (or number of FP per gram). When applied to FP lots used in the past two MRI programs the following efficiencies and equivalent sampling rates are obtained:

	FP No./gram	Metronics Efficiency	- Sampling Rate
Contract 504	1.24×10^{10}	63.3%	26.1 liters/min
545	2.16×10^{10}	58.4	24.1

FP number assessments used in the above table are laboratory-determined with highly efficient aerosolization. In the two MRI programs, however, disseminator efficiency was assumed to be 39% with consequent reduction in number per gram and increase in average particle size. If the FP numbers per gram given above are reduced to 39% of the laboratory values the following efficiencies and sampling rates are obtained:

	Corrected for 39% Disseminator Efficiency		
	FP No./gram	Metronics Efficiency	- Sampling Rate
Contract 504	$.48 \times 10^{10}$	71.0% (est.)	29.3 liters/min
545	$.84 \times 10^{10}$	66.5%	27.5

It is to be noted that the small number of particles obtained after correcting for disseminator efficiency necessitates the use of the extreme end of Metronics chart where the experimentally determined values were obviously more uncertain. In addition, it is not clear from the Metronics report that 100% aerosolization efficiency (compared to laboratory values) was achieved by the Metronics disseminator. If not, adjustment of the data to account for 39% disseminator efficiency would overcorrect the situation.

Data obtained from MRI Contracts 504 and 545 have been separately treated by least squares regression techniques, using all 53 pairs of data from each program. In addition, arithmetic mean comparisons have also been made. These data are shown in the following table:

	Effective Rotorod Sampling Rates		
	Least Squares Value	Mean Value	Corr. Metronics Rate
Contract 504	31.4 liters/min	35.2 liters/min	29.3 liters/min
545	27.3	29.6	27.5

These data are in fair agreement but there appears to be a tendency for larger effective sampling rates to appear in the MRI field data. This is particularly true when it is considered that the Metronics efficiencies are obtained by averaging test values in a manner analogous to the MRI mean value in the above table. This tendency, if real, may be due to abnormal FP size distribution as apparently experienced by Metronics during one test. Alternatively, the value of the aircraft FP disseminator efficiency may be in error. A large error in

aircraft disseminator efficiency would be required, however, to change the effective sampling rate substantially.

For the purposes of the present program an effective rotorod sampling rate of 27.3 liters per minute has been used. This is the value established from in-field measurements and closely compares with the Metronics corrected value.

APPENDIX B

AIRCRAFT TURBULENCE MEASUREMENTS

A. Turbulence Meter

In the inertial subrange of eddy sizes, the turbulent energy spectrum of longitudinal velocity fluctuations is:

$$E(k) = C_2 \, \epsilon^{2/3} \, k^{-5/3} \tag{1}$$

where ϵ is the turbulent dissipation rate, k is wave number, and C_2 is a dimensionless constant whose most recent values cluster near 0.2.

When the energy measuring probe has a velocity U_o with respect to the eddies, wave number can be converted to frequency ($k = U_o f$) and Eq. (1) becomes

$$E(f) = C_2 \, \epsilon^{2/3} \, U_o^{2/3} \, f^{-5/3} \tag{2}$$

In measuring turbulent energy from an aircraft, Eq. (2) indicates that the energy will be a function of flight speed and range of frequencies involved as well as ϵ, the dissipation rate. Of these parameters only ϵ is a fundamental turbulence parameter and it becomes essential to extract its value from the measurements by means of Eq. (2).

In practice, E(f) is measured by mounting a small propeller on the aircraft. The voltage generated by the propeller provides a measure of U_o and fluctuations about the mean propeller speed provide a measure of the turbulent fluctuations. Filters applied to the fluctuating signal have characteristics (1 - 6 cps band-pass) which assure a frequency range in the inertial subrange. The RMS value of the fluctuating signal is obtained by averaging the rectified signal and assuming a Gaussian distribution about the mean flight speed. From Eq. (2) this RMS value of the longitudinal energy fluctuations is proportional to $\epsilon^{1/3} \, U_o^{1/3}$ for a specified frequency range.

The voltage generated by the propeller is a linear function of airspeed. If this signal is processed directly by the band-pass filter, the resultant output (RMS value) would be a function of $U_o^{1/3}$. However if the propeller voltage is transmitted to the filter as:

$$\text{Voltage} \sim U_o^{2/3}$$

then voltage fluctuations (ΔV) would be related to velocity fluctuations in the following manner:

$$\Delta V \sim \frac{\Delta U_o}{U_o^{1/3}}$$

If the voltage fluctuations are now processed by the band-pass filter as described above, they may be considered to be velocity fluctuations if the factor $U_o^{-1/3}$ is included. This removes the functional dependence of the filter output on $U_o^{1/3}$ and makes it possible to record $\epsilon^{1/3}$ directly. In the turbulence meter itself, the propeller voltage is passed through a non-linear element ($\sim U_o^{2/3}$) and thence through the band-pass filter so that the meter output is no longer a function of aircraft speed and shows $\epsilon^{1/3}$ directly.

In isotropic turbulence the cross flow component of the energy spectrum is given by:

$$G(f) = \frac{4}{3} E(f) = \frac{4}{3} C_2 U_o^{2/3} \epsilon^{2/3} f^{-5/3} \tag{3}$$

Eq. (3) provides a means of obtaining the lateral velocity fluctuations (comparable to bivane measurements) from the longitudinal fluctuations recorded by the airplane. The assumption of isotropic turbulence is customary for the small eddy sizes involved in the inertial subrange. Anistropic effects are generally only associated with the larger eddy sizes.

B. Relation between ϵ and σ_τ

In order to use the results of the aircraft measurements it is necessary to relate the value of ϵ to the more familiar turbulence parameters measured by ground based instrumentation. The bivane measures the angle formed by the vector sum of the crosswind turbulent component and the mean wind or:

$$\theta = \frac{v}{U_o} \tag{4}$$

where θ is the angle involved in sigma meter calculations.

$$\overline{v^2} = \int_0^\infty G(f)\, df \tag{5}$$

by definition of power spectral density.

And so

$$\overline{\theta^2} = \sigma^2 = U_o^{-2} \int_0^\infty G(f)\, df \tag{6}$$

If the spectrum is processed by a high pass filter with a characteristic sample time τ corresponding to a filter admittance factor $A(f)$

$$\sigma_\tau^2 = U_o^{-2} \int_0^\infty A^2(f)\, G(f)\, df \tag{7}$$

Substituting (3) in (7),

$$\sigma_\tau^2 = \frac{4}{3} C_2 \, U_o^{-4/3} \, \epsilon^{2/3} \int_0^\infty A^2 (f) \, f^{-5/3} \, df \tag{8}$$

The integral can be found most simply by graphical integration, using the known A(f) curves as shown in Appendix B of MRI61 FR-33 on the Dallas Tower Program, or as given in Jones and Pasquill (9).

Where σ is recorded in degrees instead of radians, an additional 57.3 factor is required. With C_2 set at 0.2, and for 2.5 second sampling time, it turns out that (8) reduces to

$$\epsilon = 1.15 \times 10^{-2} \, \sigma_{2.5}^{3} \, U_o^{3} \qquad \text{for } \epsilon \text{ in cm}^2 \text{ sec}^{-3}, \; U_o \text{ in mph}, \; \sigma_{2.5} \text{ in degrees} \tag{9}$$

or

$$\epsilon^{1/3} = 0.226 \, \sigma_{2.5} \, U_o^{3/3} \tag{10}$$

Similarly, one finds

$$\epsilon^{1/3} = .181 \, \sigma_5 \, U_o^{3/3} \tag{11}$$

for a 5-second sampling time on the sigma meter.

The derivation above is only valid as long as the eddies contributing to the sigma meter lie exclusively in the inertial subrange. This will be generally true if the eddies passing the filter are shorter than the height (see MacCready, (1). For a sigma meter filter, $A^2 < .5$, for $f > 0.44/\tau$. For $\tau = 2.5$ seconds, this is at 0.176 cps. Thus, the criterion for validity of (10) can be given as

$$U_o < 0.176 \, z$$

and the criterion for validity of (11) can be given as

$$U_o < 0.088 \, z \, .$$

For the heights employed in the Dallas Tower Program,

Height	U_o maximum for ϵ calculation from $\sigma_{2.5}$	U_o maximum for ϵ calculation from σ_5
30 ft.	3.6 mph	1.8 mph
150	18	9
300	36	18
450	54	27
750	92	46
1050	126	63

Usually the calculation will still be reasonably valid even for winds somewhat over twice as strong as those shown above. Where both (10) and (11) are valid, it will be found theoretically that

$$\sigma_s = 1.25\ \sigma_{s.s}$$

Because of the dynamic overshoot of the direction vane, each sigma meter reading will be slightly higher than the true value, but even in the extreme cases this should be less than 10% and so it is ignored here. When the winds are strong enough at low altitudes to cause the σ_s reading or the σ_s and $\sigma_{s.s}$ readings to depend on eddies beyond the inertial subrange, then the ratio of $\sigma_s/\sigma_{s.s}$ would be expected to be less than 1.25, although, of course, always greater than 1.

Thus, for the purposes of the present program, if $\epsilon^{1/3}$ is measured directly from the aircraft and U_o is obtained from pibal measurements, σ_s at the aircraft flight level can be obtained from Eq. (11).

APPENDIX C

DATA SUMMARY

Trial No.	Date	Time Local	Release Height ft.	Avg. Wind To Release mph	Effective Turb. i_e deg.
Oklahoma					
1	6-4	1813	500	15	2.85
2	6-4	2216	500	17	2.65
3	6-5	2042	500	15	1.5
4	6-14	2057	500	13	.8
5	6-15	1952	500	12	2.3
6	6-15	2342	500	13	2.95
7	6-16	0348	500	15	3.0
8	6-16	2005	500	17	3.2
9	6-16	2310	500	16	2.85
Texas					
11	6-24	1612	500	19	1.3
12	6-24	2009	500	12	1.4
13	6-25	0001	500	16	1.0
14	6-27	1944	500	17	1.2
15	6-28	1938	750	18	1.1
16	6-28	2338	500	14	1.2
17	6-29	1928	1000	16	.85
18	6-29	2337	500	15	1.3
19	6-29	0328	500	15	1.6
Washington					
20	10-2	2215	1200	-	1.65
21	10-6	1452	1200	13	2.3
22	10-6	1807	1200	16	3.0
23	10-6	2219	1200	21	.55
24	10-7	0136	1200	17	1.15
25	10-15	1816	1200	16	2.9
26	10-21	1453	1200	19	2.55
27	10-21	1805	1200	16	.95
28	10-21	2218	1200	22	.50
Nevada					
29	10-31	1555	1300	14	2.25
30	10-31	1918	1300	18	.70
31	11-1	1908	1300	15	1.4
32	11-1	2202	1300	13	1.85
33	11-2	0202	1300	11	3.3
34	11-4	1733	1300	-	3.9
35	11-5	1903	1300	21	2.4
36	11-5	2154	1300	18	2.35

APPENDIX C

DATA SUMMARY

(cont.)

Trial	Direction	100 ft. Velocity (mph)	100 ft. σ_{180} (deg.)	100 ft. σ_5 (deg.)	30 ft. Velocity (mph)	30 ft. σ_{180} (deg.)	30 ft. σ_5 (deg.)	Temperature 30 ft. (°C)	Temperature 30-100 ft. (°C)
Oklahoma									
1	S	10.2	8.0	---	7.4	---	---	25.0	-.1
2	SSE	11.0	10.7	---	8.2	---	---	22.5	-.3
3	S	10.8	8.1	6.2	7.7	9.5	6.2	24.3	-.4
4	SE	8.4	4.3	3.1	5.4	5.1	4.4	19.3	.2
5	SE	9.2	7.1	4.6	7.5	7.1	5.5	22.7	-.2
6	SE	9.1	8.0	5.7	7.4	8.2	6.3	20.2	-.3
7	SSE	10.0	9.0	5.6	8.3	8.7	6.5	17.1	-.2
8	SSE	12.4	7.0	5.2	10.3	7.1	6.1	24.4	-.3
9	SSE	13.4	7.6	5.1	11.4	8.9	6.6	22.7	-.1
Texas									
11	ESE	23.5	3.1	1.9	20.2	5.4	4.7	26.5	-1.0
12	SE	9.6	4.2	2.2	7.2	6.2	5.1	24.0	-.3
13	SSE	12.8	3.5	2.7	9.4	7.1	5.8	23.9	-.3
14	ESE	11.0	2.5	---	9.0	3.7	---	24.5	-.7
15	SE	12.3	3.9	3.7	9.0	6.1	5.0	24.5	-.6
16	SE	10.6	3.9	2.9	7.8	6.1	4.9	24.1	-.5
17	SE	12.4	5.6	---	8.8	---	---	24.1	-.4
18	SE	11.1	6.7	---	8.3	---	---	24.0	-.3
19	SSE	12.9	6.3	---	7.8	---	---	23.8	-.2
Washington									
20	SW	38.0	5.1	3.7	29.0	5.3	5.1	12.4	.25
21	SSE	16.0	3.5	2.0	13.0	4.7	4.2	10.4	.4
22	S	9.0	6.2	4.2	6.0	8.0	5.4	8.5	.2
23	SSE	5.0	3.7	4.0	3.0	4.2	4.2	5.7	-.5
24	SSE	7.0	3.6	2.1	5.0	4.0	2.3	3.9	-.25
25	SSW	6.4	1.8	1.3	1.0	3.6	3.1	5.5	-.5
26	SW	10.8	4.7	2.7	4.2	5.2	3.9	14.2	.5
27	SSW	2.8	3.2	0.8	---	5.1	1.1	10.3	-.7
28	SSW	9.0	1.2	0.7	5.6	3.9	3.2	6.3	-1.5
Nevada									
29	NNW	8.0	4.8	---	6.9	---	---	18.4	.5
30	NNW	7.2	3.0	2.4	6.2	3.1	2.7	12.7	-.4
31	N	12.4	3.8	2.0	10.0	4.5	3.3	13.6	-1.15
32	N	7.2	1.3	0.7	6.0	4.5	2.1	11.8	-.15
33	N	4.6	2.2	1.6	3.8	2.3	1.6	9.0	0
34	NE	2.2	---	---	c	---	---	12.4	-1.5
35	N	18.0	3.8	3.4	15.0	3.9	3.7	9.5	-.25
36	N	11.2	3.5	2.5	8.0	3.7	2.9	7.7	-.25

DATA SUMMARY

UPPER WIND SUMMARY (MPH)

Trial	Date	Time	Elevation 230 ft	675 ft	1100 ft	1520 ft	2135 ft	2940 ft	3735 ft
Oklahoma									
1	6-4-62	1815	14.7	18.0	19.8	21.0	20.6	19.0	25.0
2	6-4-62	2215	17.3	31.0	42.1	43.2	44.5		
3	6-5-62	2130	14.9	28.9	34.1	34.1	35.4	31.8	
4	6-14-62	2115		19.1	24.7	23.0	24.8	23.4	24.0
5	6-15-62	2015	15.5	27.9	34.6	36.2	36.0		
6	6-15-62	2400	12.6	25.2	38.9	41.9	41.7		
7	6-16-62	0530	13.5	30.1	46.4	53.8	50.2	45.6	
8	6-16-62	2125	14.5	27.2	39.2	48.1	49.4		
9	6-16-62	2350	15.7	30.6	42.7	50.2	54.6		
Texas									
11	6-24-62	1630		26.1	18.5	23.2	16.6		
12	6-24-62	2025	12.2	10.8	10.6	17.6	25.1	26.1	22.5
13	6-25-62	0030		18.9	15.7	14.8	17.0	18.8	16.9
14	6-27-62	2000	16.7	18.0	16.4	14.9	16.1		
15	6-28-62	2000	16.3	21.8	16.0	25.6	18.0	17.9	19.2
16	6-28-62	2400			14.2	16.4	15.4	19.3	17.3
17	6-29-62	2030	16.5	17.5	17.6	16.6	14.3	13.3	14.6
18	6-30-62	0005	14.8	17.6	19.6	18.5	20.9	24.4	
19	6-30-62	0400		19.1	22.1	21.8	21.2	27.7	

DATA SUMMARY

UPPER WIND SUMMARY (MPH)

Trial	Date 1962	Time	Elevation (ft) 200	380	580	930	1270	1610	1945	2275	2605	2935	3260
Washington													
21	10-6	1439	13.0		14.0	12.0	15.0	13.0	18.0	20.0	20.0	21.0	29.5
22	10-6	1750		15.0		17.5	19.0	21.5					
23	10-6	2230		16.0		30.0	31.0	29.0	27.0				
24	10-7	0157	13.5		19.0								
25	10-15	1830	12.0		18.0	18.0	21.0	19.0	17.0	19.0			
26	10-21	1510	15.0		20.0	21.0	19.0	18.5	19.5	18.0	20.5	23.0	25.0
27	10-21	1825	7.0		19.0	23.0	24.0	23.0	27.0				
28	10-21	2240		16.0		31.0	29.0	28.0					
Nevada													
29	10-31	1647	14.0		17.0	20.0	20.0	20.5	23.0	21.0	23.0	20.0	13.0
30	10-31	2032	18.0		24.0	33.0	38.0	39.0	43.0	27.0	27.0	19.0	24.0
31	11-1	2000	15.0		25.0	26.5	19.0	14.0	13.0	11.0	12.0		
32	11-1	2305	13.0		21.0	20.0	12.0	11.0	13.0	10.5	9.5	9.0	
33	11-2	0310	11.0		11.5	6.5	3.0	3.5	3.5	13.0	4.0	9.0	9.0
34	11-4	1800		4.0		3.0	3.5		5.5	6.5	3.5	7.0	3.0
35	11-5	1925		28.0		40.0	38.0	37.0	33.0				
36	11-5	2225		24.0		38.0	43.0	38.0	33.0	26.0	27.5		

DOSAGES

OKLAHOMA

TRIAL 1

Roto-rod No.	Distance from Release	Dosage* Obs.	Dosage* Cal.
1	4.0 mi.	60.6(?)	1.0
2	5.0	3.4	4.9
3	5.9	12.9	10.6
4	6.8	32.9	16.2
5	7.8	34.5	21.5
6	9.1	24.2	26.4
7	10.1	25.3	28.6
8	11.2	32.3	30.0
9	12.2	48.6	30.4
10	13.1	.1	30.5
11	14.2	37.0	30.2
12	15.7	33.4	29.4
13	16.7	30.8	28.7
14	17.6	28.2	28.0
15	18.6	32.3	27.3
16	19.9	44.9	26.3
17	20.9	34.6	25.5
18	22.1	27.2	24.6
19	23.1	22.0	23.9
20	24.0	20.7	23.2
21	24.9	20.1	22.6
22	26.3	16.3	21.7
23	27.3	12.2	21.1
24	28.3	10.3	20.5
25	29.3	9.1	20.0

TRIAL 2

Roto-rod No.	Distance from Release	Dosage* Obs.	Dosage* Cal.
1	3.3 mi.	6.1	
2	4.2	.9	.2
3	5.1	10.6	1.6
4	6.2	24.2	5.0
5	7.1	49.6	8.7
6	8.4	67.2	13.6
7	9.4	65.3	16.6
8	10.5	47.4	18.9
9	11.5	27.1	20.3
10	12.5	.1	21.3
11	13.6	29.2	21.8
12	15.0	27.0	22.0
13	16.1	23.8	21.7
14	17.0	22.8	21.5
15	17.9	27.2	21.2
16	19.3	28.7	20.6
17	20.4	26.1	20.1
18	21.5	26.9	19.6
19	22.5	25.7	19.1
20	23.4	27.2	18.7
21	24.4	26.6	18.1
22	25.7	25.7	17.6
23	26.8	22.2	17.1
24	27.8	19.9	16.7
25	28.8	22.1	16.2

*Dosage in particles-min/liter

Effective source strength 3.64×10^9 particles/meter

DOSAGES

OKLAHOMA

TRIAL 3

Roto-rod No.	Distance from Release	Dosage* Obs.	Dosage* Cal.
1	4.1 mi.	1.8	
2	5.1	.1	
3	6.0	1.4	
4	7.1	2.1	
5	8.0	8.0	
6	9.4	8.1	.1
7	10.4	11.1	.4
8	11.5	16.3	1.0
9	12.5	16.3	2.0
10	13.5	.1	3.3
11	14.7	21.9	5.2
12	16.0	26.9	7.6
13	17.2	23.8	9.9
14	18.1	26.6	11.6
15	19.0	27.3	13.2
16	20.4	29.0	15.5
17	21.5	30.9	17.3
18	22.7	34.9	18.8
19	23.7	31.9	19.9
20	24.6	38.0	20.8
21	25.7	35.8	21.8
22	27.1	40.2	22.7
23	28.1	29.3	23.4
24	29.1	20.5	23.9
25	30.1	27.7	24.2

TRIAL 4

Roto-rod No.	Distance from Release	Dosage* Obs.	Dosage* Cal.
1	2.6 mi.	2.6	Less than .1
2	3.5	0	
3	4.5	0	
4	5.4	0	
5	6.4	0	
6	7.7	.2	
7	8.7	0	
8	9.9	1.2	
9	10.8	4.7	
10	11.8	.4	
11	12.9	3.1	
12	14.5	4.5	
13	15.6	6.0	
14	16.6	4.4	
15	17.5	6.4	
16	18.9	38.1	
17	19.9	59.5	
18	21.1	54.8	
19	22.1	73.0	
20	23.0	42.3	
21	24.0	22.8	
22	25.3	10.4	
23	26.4	27.5	
24	27.4	42.4	
25	28.4	35.0	

*Dosage in particles-min/liter

Effective source strength 3.64×10^9 particles/meter

DOSAGES

OKLAHOMA

TRIAL 5

Roto-rod No.	Distance from Release	Dosage* Obs.	Dosage* Cal.
1	2.0 mi.	3.6	
2	2.8	12.5	
3	3.8	8.2	
4	4.7	16.6	
5	5.6	18.7	.4
6	6.9	29.7	2.4
7	7.9	21.0	5.3
8	8.9	19.2	9.2
9	9.8	46.7	12.6
10	10.8	1.9	16.3
11	11.9	68.0	19.7
12	13.4	78.6	23.4
13	14.5	34.5	25.4
14	15.4	23.8	26.5
15	16.3	26.2	27.4
16	17.6	25.9	28.1
17	18.7	20.6	28.4
18	19.7	18.9	28.4
19	20.7	36.6	28.4
20	21.6	40.3	28.0
21	22.6	33.0	27.9
22	23.8	38.5	27.4
23	24.9	47.2	26.9
24	25.8	31.0	26.7
25	26.8	50.1	26.2

TRIAL 6

Roto-rod No.	Distance from Release	Dosage* Obs.	Dosage* Cal.
1	1.8 mi.	2.8	
2	2.7	9.9	
3	3.6	13.8	.6
4	4.5	25.2	3.6
5	5.4	48.8	8.8
6	6.6	29.2	16.1
7	7.6	32.6	21.2
8	8.8	54.2	24.7
9	9.6	62.1	26.2
10	10.6	42.0	27.2
11	11.6	57.9	27.7
12	13.1	59.8	27.6
13	14.2	54.9	26.8
14	15.1	51.1	26.4
15	16.0	45.3	25.8
16	17.2	42.5	24.9
17	18.3	40.7	24.0
18	19.4	37.2	23.2
19	20.3	28.7	22.6
20	21.2	29.4	21.9
21	22.1	32.8	21.3
22	23.3	23.5	20.5
23	24.4	18.2	19.8
24	25.4	18.0	19.3
25	26.3	17.5	18.7

*Dosage in particles-min/liter

Effective source strength 3.64×10^9 particles/meter

DOSAGES

OKLAHOMA

TRIAL 7				TRIAL 8			
Roto-rod No.	Distance from Release	Dosage* Obs.	Dosage* Cal.	Roto-rod No.	Distance from Release	Dosage* Obs.	Dosage* Cal.
1	2.4 mi.	59.6		1	2.5 mi.	16.7	
2	3.2	22.2	.2	2	3.3	53.9	1.1
3	4.1	47.4	2.4	3	4.2	12.9	5.2
4	5.0	17.4	7.1	4	5.1	31.8	10.8
5	5.9	55.8	12.7	5	6.0	34.7	15.9
6	7.1	59.7	19.1	6	7.2	6.1	20.5
7	8.1	37.7	23.0	7	8.2	13.1	22.7
8	9.2	51.0	25.3	8	9.2	8.4	23.7
9	10.1	48.2	26.3	9	10.1	10.2	23.9
10	11.0	48.1	26.7	10	11.1	16.2	23.7
11	12.1	36.1	26.7	11	12.2	28.9	23.2
12	13.6	34.4	26.1	12	13.6	28.5	22.2
13	14.6	34.4	25.5	13	14.7	26.9	21.4
14	15.5	38.0	24.9	14	15.6	34.2	20.7
15	16.3	47.8	24.3	15	16.5	42.1	20.0
16	17.7	44.3	23.3	16	17.8	41.1	19.0
17	18.6	42.0	22.6	17	18.7	36.2	18.4
18	19.8	40.3	21.7	18	19.8	39.0	17.7
19	20.7	34.0	21.0	19	20.8	45.7	17.0
20	21.6	27.4	20.4	20	21.7	33.6	16.5
21	22.5	31.4	19.8	21	22.6	39.7	16.0
22	23.8	32.8	19.0	22	23.8	26.0	15.3
23	24.8	27.2	18.5	23	24.9	13.2	14.8
24	25.7	18.7	17.9	24	25.8	7.8	14.3
25	26.6	18.6	17.6	25	26.7	7.7	13.9

*Dosage in particles-min/liter

Effective source strength 3.64×10^{9} particles/meter

DOSAGES

OKLAHOMA

TRIAL 9

Roto-rod No.	Distance from Release	Dosage* Obs.	Dosage* Cal.
1	2.4 mi.	6.2	
2	3.3	8.2	.1
3	4.2	12.7	1.2
4	5.1	13.5	4.3
5	6.0	17.8	8.7
6	7.2	23.0	14.5
7	8.2	19.6	18.2
8	9.2	29.4	20.8
9	10.1	30.3	22.4
10	11.1	29.6	23.3
11	12.1	29.2	23.7
12	13.6	23.6	23.7
13	14.6	31.1	23.4
14	15.6	36.7	23.0
15	16.4	34.7	22.6
16	17.7	36.8	21.8
17	18.7	30.4	21.2
18	19.8	28.1	20.4
19	20.7	26.9	20.0
20	21.6	26.2	19.5
21	22.5	23.2	19.0
22	23.7	21.9	18.3
23	24.9	19.4	17.7
24	25.8	23.2	17.2
25	26.7	23.0	16.8

TEXAS

TRIAL 11

Roto-rod No.	Distance from Release	Dosage* Obs.	Dosage* Cal.
1	4.5 mi.	18.6	
2	5.1	12.3	
3	6.0	28.7	
4	6.9	.1	
5	7.7	2.5	
6	8.9	0	
7	9.9	4.0	
8	11.7	8.7	
9	12.7	12.1	
10	13.6	4.3	
11	14.5	7.2	
12	15.3	11.1	
13	16.3	5.4	.1
14	17.2	10.6	.2
15	18.0	5.3	.4
16	18.5	9.6	.5
17	19.5	5.9	.8
18	20.5	7.0	1.3
19	21.4	7.9	1.9
20	22.4	No rotorod	2.4
21	23.4	7.9	3.2
22	24.5	8.2	4.1
23	25.4	6.3	4.9
24	26.7	4.8	6.2
25	27.5	4.5	7.0

*Dosage in particles-min/liter

Effective source strength 3.64×10^9 particles/meter

DOSAGES

TEXAS

TRIAL 12				TRIAL 13			
Roto-rod No.	Distance from Release	Dosage* Obs.	Dosage* Cal.	Roto-rod No.	Distance from Release	Dosage* Obs.	Dosage* Cal.
1	4.9 mi.	42.8		1	6.1 mi.	26.8	
2	5.7	16.6		2	7.1	23.5	
3	6.6	10.7		3	8.3	11.1	
4	7.5	8.7		4	9.5	20.3	
5	8.5	25.0		5	10.6	23.9	
6	9.7	5.9		6	12.3	8.6	
7	11.0	21.0		7	13.8	3.5	
8	12.8	25.6		8	16.0	.8	
9	13.9	14.8	.2	9	17.5	1.8	
10	14.9	14.3	.4	10	18.7	6.4	
11	15.9	18.7	.8	11	19.8	2.9	
12	16.8	7.6	1.3	12	21.0	15.3	
13	17.9	8.8	2.2	13	22.5	10.2	
14	18.9	21.9	3.3	14	23.6	6.8	
15	19.7	9.2	4.3	15	24.6	13.5	
16	20.4	12.2	5.4	16	25.5	15.5	
17	21.5	18.4	7.1	17	26.8	.8	.1
18	22.5	18.2	8.8	18	28.1	.2	.2
19	23.5	12.3	10.6	19	29.3	.1	.3
20	24.6	9.2	12.7	20	30.6	0	.5
21	25.7	10.8	14.8	21	32.2	.1	.8
22	26.9	9.4	17.0	22	33.6	.3	1.2
23	27.9	13.1	18.6	23	34.9	.6	1.7
24	29.4	11.3	21.3	24	36.8	.2	2.5
25	30.2	13.6	22.4	25	37.9	.2	3.0

*Dosage in particles-min/liter

Effective source strength 3.64×10^9 particles/meter

DOSAGES

TEXAS

TRIAL 14

Roto-rod No.	Distance from Release	Dosage* Obs.	Dosage* Cal.
1	2.8 mi.	64.1	
2	3.4	72.5	
3	4.3	22.4	
4	5.2	56.3	
5	6.0	5.2	
6	7.2	77.0	
7	8.3	56.7	
8	9.9	34.9	
9	11.0	31.3	
10	11.9	31.5	
11	12.7	7.0	
12	13.6	.1	
13	14.6	.3	
14	15.4	.1	
15	16.2	.1	
16	16.7	.4	
17	17.7	.4	
18	18.7	.4	.1
19	19.6	.2	.2
20	20.6	.2	.3
21	21.6	1.7	.5
22	22.7	.3	.8
23	23.5	.1	1.1
24	24.9	0	1.8
25	25.7	0	2.3

TRIAL 15

Roto-rod No.	Distance from Release	Dosage* Obs.	Dosage* Cal.
1	2.9 mi.	78.9	Less than .1
2	3.6	17.6	
3	4.5	72.2	
4	5.5	No rotorod	
5	6.2	27.3	
6	7.6	36.0	
7	8.7	14.4	
8	10.4	34.3	
9	11.6	.1	
10	12.5	28.2	
11	13.3	24.5	
12	14.3	10.3	
13	15.3	15.8	
14	16.2	15.2	
15	17.0	10.3	
16	17.6	11.4	
17	18.6	18.1	
18	19.6	19.3	
19	20.6	20.5	
20	21.6	32.8	
21	22.7	29.1	
22	23.7	28.8	
23	24.7	13.0	
24	26.2	11.8	
25	27.0	24.2	

*Dosage in particles-min/liter

Effective source strength 3.64×10^9 particles/meter

DOSAGES

TEXAS

TRIAL 16

Roto-rod No.	Distance from Release	Dosage* Obs.	Dosage* Cal.
1	2.9 mi.	47.1	
2	3.6	24.1	
3	4.6	28.4	
4	5.5	18.1	
5	6.3	7.2	
6	7.6	.9	
7	8.7	20.0	
8	10.5	26.8	
9	11.6	34.4	
10	12.6	22.2	
11	13.4	11.4	
12	14.3	8.3	
13	15.4	6.4	
14	16.3	14.4	
15	17.0	9.8	
16	17.6	6.7	
17	18.7	12.2	.1
18	19.7	9.9	.2
19	20.7	11.9	.4
20	21.6	28.3	.6
21	22.7	33.6	1.0
22	23.8	37.0	1.5
23	24.7	23.6	2.1
24	26.2	7.3	3.1
25	27.0	16.6	3.8

TRIAL 17

Roto-rod No.	Distance from Release	Dosage* Obs.	Dosage* Cal.
1	3.1 mi.	1.4	Less than .1
2	3.8	.7	
3	4.8	2.3	
4	5.8	15.4	
5	6.6	30.0	
6	7.9	19.7	
7	9.2	8.4	
8	10.9	34.9	
9	12.1	48.3	
10	13.1	34.5	
11	14.0	36.3	
12	14.9	15.8	
13	16.0	17.0	
14	16.9	25.9	
15	17.8	9.5	
16	18.4	11.6	
17	19.5	13.8	
18	20.6	34.8	
19	21.6	24.4	
20	22.6	44.5	
21	23.7	30.6	
22	24.8	25.1	
23	25.9	20.1	
24	27.4	15.6	
25	28.2	34.7	

*Dosage in particles-min/liter

Effective source strength 3.64×10^9 particles/meter

DOSAGES

TEXAS

TRIAL 18

Roto-rod No.	Distance from Release	Dosage* Obs.	Dosage* Cal.
1	3.3 mi.	57.4	
2	4.0	8.7	
3	5.1	38.9	
4	6.1	18.5	
5	7.0	14.9	
6	8.4	5.5	
7	9.7	51.9	
8	11.5	20.0	
9	12.7	8.2	
10	13.7	28.6	
11	14.7	12.5	
12	15.7	8.1	.1
13	16.8	12.9	.2
14	17.8	6.6	.4
15	18.7	8.2	.7
16	19.3	10.8	1.0
17	20.5	24.4	1.6
18	21.6	13.3	2.4
19	22.7	13.2	3.4
20	23.7	26.4	4.3
21	25.0	11.3	5.8
22	26.2	14.0	7.2
23	27.3	22.1	8.6
24	28.8	17.3	10.5
25	29.6	7.4	11.4

TRIAL 19

Roto-rod No.	Distance from Release	Dosage* Obs.	Dosage* Cal.
1	4.0 mi.	38.6	
2	4.8	35.9	
3	6.2	82.5	
4	7.4	45.4	
5	8.5	9.6	
6	10.3	27.4	.1
7	11.9	19.8	.5
8	14.2	14.0	2.3
9	15.7	41.7	4.4
10	17.0	11.0	6.6
11	18.2	23.3	8.9
12	19.5	18.3	11.4
13	20.8	10.5	13.9
14	22.2	18.5	16.4
15	23.3	21.3	18.4
16	23.9	22.7	19.1
17	25.5	16.6	21.5
18	26.9	38.2	22.9
19	28.2	34.3	24.5
20	29.5	45.3	25.4
21	31.1	44.5	26.6
22	32.6	14.3	27.4
23	34.0	.5	27.9
24	35.9	0	28.4
25	37.0	0	28.7

*Dosage in particles-min/liter

Effective source strength 3.64×10^9 particles/meter

DOSAGES

WASHINGTON

TRIAL 20

Roto-rod No.	Distance from Release	Dosage* Obs.	Dosage* Cal.
1	-1.6 mi.	.3	None
2	-0.8	.1	
3	0.1	.1	
4	1.0	.3	
5	2.0	.3	
6	3.0	.2	
7	3.9	.6	
8	4.9	.6	
9	5.7	.7	
10	6.3	--	
11	7.2	.2	
12	8.4	.1	
13	9.4	.5	
14	10.4	0	
15	11.3	.1	
16	12.2	.2	
17	13.2	.1	
18	14.2	0	
19	15.2	.2	
20	15.8	.2	
21	17.2	.1	
22	18.2	.1	
23	19.1	.3	
24	20.1	.2	
25	21.0	.2	

Rosalia Sampler Line

*Dosage in particles-min/liter

Effective source strength 3.64×10^9 particles/meter

TRIAL 21

Roto-rod No.	Distance from Release	Dosage* Obs.	Dosage* Cal.
1	-1.6 mi.	1.5	
2	-0.9	.2	
3	-0.2	.4	
4	0.6	.2	
5	1.6	.3	
6	2.5	.2	
7	3.3	.3	
8	3.6	.2	
9	4.1	.1	
10	5.2	2.9	
10T	5.9	1.1	
11	6.4	6.0	
12	6.9	2.1	
13	7.6	4.4	
14	8.7	18.1	
15	9.6	11.5	
16	10.5	5.6	
17	11.6	.4	
18	12.6	6.6	.1
19	13.6	9.0	.2
20	14.7	2.3	.4
21	15.5	.6	.7
22	15.9	---	.9

Tekoa Sampler Line
10T - 100 ft. Tower Location
*Dosage in particles-min/liter

Effective source strength 3.64×10^9 particles/meter

DOSAGES

WASHINGTON

TRIAL 22

Roto-rod No.	Distance from Release	Dosage* Obs.	Dosage* Cal.
1	-1.5 mi.	1.8	
2	-0.9	2.6	
3	-0.1	.7	
4	0.6	.9	
5	1.6	1.3	
6	2.5	.7	
7	3.2	1.7	
8	3.5	.7	
9	3.9	.6	
10	4.9	1.0	
10T	5.8	8.0	
11	6.2	4.3	
12	6.5	---	
13	7.2	1.6	
14	8.3	3.3	.2
15	9.1	3.6	.6
16	9.9	2.1	1.1
17	11.0	3.0	2.0
18	12.1	4.7	3.1
19	13.0	8.3	4.2
20	14.2	8.3	5.5
21	14.9	3.4	6.2
22	15.3	3.8	6.6

TRIAL 23

Roto-rod No.	Distance from Release	Dosage* Obs.	Dosage* Cal.
1	-2.0 Mi.	.3	Less
2	-1.0	.1	than .1
3	-0.1	.3	
4	0.8	.3	
5	1.9	.1	
6	2.8	.2	
7	3.7	.4	
8	4.4	.1	
9	5.4	.2	
10	6.5	.5	
10T	5.6	.1	
11	7.7	.3	
12	8.7	.3	
13	9.7	.1	
14	10.8	.3	
15	11.9	.7	
16	13.0	.5	
17	14.1	.3	
18	14.9	.3	
19	15.5	.8	
20	16.7	.1	
21	17.8	.1	
22	18.7	.6	

Tekoa Sampler Line
10T - 100 ft. Tower Location

*Dosage in particles-min/liter

Effective source strength 3.64 x 10^9 particles/meter

DOSAGES

WASHINGTON

TRIAL 24

Roto-rod No.	Distance from Release	Dosage* Obs.	Dosage* Cal.
1	-1.3 mi.	.4	Less
2	-0.6	.3	than .1
3	0.2	.3	
4	0.9	.4	
5	1.9	.4	
6	2.8	.2	
7	3.6	.7	
8	3.9	.3	
9	4.5	.1	
10	5.6	.1	
10T	6.3	4.7	
11	6.7	.3	
12	7.3	.3	
13	7.9	2.4	
14	9.1	.7	
15	9.9	5.6	
16	10.9	8.8	
17	12.0	5.5	
18	12.9	.2	
19	13.9	2.7	
20	15.2	2.2	
21	15.9	---	
22	16.3	7.1	

TRIAL 25

Roto-rod No.	Distance from Release	Dosage* Obs.	Dosage* Cal.
1	0.5 mi.	.1	
2	1.5	.1	
3	2.0	.5	
4	2.8	.3	
5	3.6	.1	
6	4.2	.2	
7	4.9	.6	
8	5.8	.5	
9	6.7	.3	
10	7.5	.2	
10T	5.4	.6	
11	8.3	.3	.1
12	9.5	.5	.5
13	10.2	.3	.8
14	11.0	.4	1.3
15	11.9	.3	2.1
16	12.9	.5	3.1
17	13.5	1.0	3.7
18	12.8	.4	3.0
19	13.7	0	3.9
20	14.5	.9	4.8
21	15.7	.6	5.9
22	16.5	.2	6.7

Tekoa Sampler Line
10T - 100 ft. Tower Location

*Dosage in particles-min/liter

Effective source strength 3.64×10^9 particles/meter

DOSAGES

WASHINGTON

TRIAL 26

Roto-rod No.	Distance from Release	Dosage* Obs.	Dosage* Cal.
1	1.6 mi.	.1	
2	2.5	3.8	
3	3.3	14.6	
4	4.2	1.4	
5	5.0	39.7	
6	5.8	9.6	
7	6.6	21.3	
8	7.4	13.1	
9	8.4	No rotorod	
10	9.4	11.7	
10T	7.4	18.7	
11	10.3	13.3	
12	11.4	17.6	.2
13	12.3	16.9	.4
14	13.2	16.9	.7
15	14.2	28.4	1.1
16	15.3	9.5	1.7
17	16.1	20.1	2.2
18	16.6	12.9	2.5
19	16.7	16.2	2.6
20	17.6	24.4	3.2
21	18.8	24.5	4.0
22	19.7	38.5	4.6

TRIAL 27

Roto-rod No.	Distance from Release	Dosage* Obs.	Dosage* Cal.
1	1.0 mi.		Less than .1
2	1.9		
3	2.5		
4	3.2		
5	4.0		
6	4.6		
7	5.5	.1	
8	6.1		
9	7.1	.1	
10	7.9		
10T	5.7		
11	8.5		
12	9.7		
13	10.5	.1	
14	11.5		
15	12.2	.1	
16	13.2		
17	13.8	.1	
18	14.2		
19	14.0		
20	14.8		
21	15.9		
22	16.8		

Tekoa Sampler Line
10T - 100 ft. Tower Location

*Dosage in particles-min/liter

Effective source strength 3.64 x 10^9 particles/meter

DOSAGES

WASHINGTON

TRIAL 28

Roto-rod No.	Distance from Release	Dosage* Obs.	Dosage* Cal.
1	1.2 mi.		Less
2	2.1		than .1
3	2.6		
4	3.4		
5	4.2		
6	4.9		
7	5.6		
8	6.4		
9	7.3		
10	8.1		
10T	5.9		
11	8.9		
12	10.0		
13	10.8		
14	11.6	.1	
15	12.5		
16	13.4		
17	14.1		
18	14.5		
19	14.4		
20	15.1	.1	
21	16.3	.1	
22	17.7		

Tekoa Sampler Line
10T - 100 ft. Tower Location

*Dosage in particles-min/liter

Effective source strength
3.64×10^9 particles/meter

NEVADA

TRIAL 29

Roto-rod No.	Distance from Release	Dosage* Obs.	Dosage* Cal.
1	-2.0 mi.	.2	
2	-1.6	No rotorod	
3	-0.2	.3	
4	0.8	29.7	
5	1.7	143.9	
6	2.7	180.4	
7	3.8	128.0	
8	4.6	73.0	
9	5.4	53.2	
10	6.3	36.3	
11	7.4	19.4	
12	8.3	22.5	
13	9.2	15.0	
14	10.2	16.1	
14 1/2	10.8	20.6	
15	11.3	21.2	
15 1/2	11.9	20.9	
16	12.3	16.9	
17	13.2	15.0	
18	14.2	10.9	.1
19	15.0	14.9	.1
20	16.0	8.1	.2
21	17.0	6.2	.5
22	18.0	11.3	.7
23	19.0	16.2	1.1
24	19.9	23.0	1.5
25	21.0	27.2	2.0

Rotorod No. 15 - Top of Ridge

*Dosage in particles-min/liter

Effective source strength
3.64×10^9 particles/meter

DOSAGES

NEVADA

TRIAL 30

Roto-rod No.	Distance from Release	Dosage* Obs.	Dosage* Cal.
1	-4.0 mi.		Less
2	-3.3		than .1
3	-2.5	.1	
4	-1.8	.9	
5	-1.1	.2	
6	-0.3		
7	0.6	.6	
8	1.2		
9	1.8	.3	
10	2.5	.4	
11	3.2	1.9	
12	4.0	2.3	
13	4.8	2.3	
14	5.7	1.6	
14 1/2	6.2	2.0	
15	6.7	1.0	
15 1/2	7.3	.2	
16	7.7	3.2	
17	8.5	4.5	
18	9.2	11.3	
19	9.8	27.9	
20	10.6	16.6	
21	11.5	11.5	
22	12.4	9.3	
23	13.3	17.5	
24	14.0	36.6	
25	14.9	16.6	

TRIAL 31

Roto-rod No.	Distance from Release	Dosage* Obs.	Dosage* Cal.
1	-0.2 mi.	.1	Less
2	0.6	.6	than .1
3	1.6	.1	
4	2.6	0	
5	3.4	.1	
6	4.5	.2	
7	5.7	.1	
8	6.6		
9	7.4	.1	
10	8.3	.4	
11	9.5	4.1	
12	10.4	10.5	
13	11.3	5.1	
14	12.4	2.6	
14 1/2	12.9	3.0	
15	13.5	3.7	
15 1/2	13.9	2.7	
16	14.5	4.6	
17	15.4	3.4	
18	16.3	7.0	
19	17.3	10.6	
20	18.3	9.2	
21	19.3	9.9	
22	20.3	10.7	
23	21.2	5.7	
24	22.3	8.7	
25	23.3	9.0	

Rotorod No. 15 - Top of Ridge

*Dosage in particles-min/liter

Effective source strength 3.64 x 10^9 particles/meter

DOSAGES

NEVADA

TRIAL 32

Roto-rod No.	Distance from Release	Dosage* Obs.	Dosage* Cal.
1	-0.6 mi.		
2	0.3	No rotorod	
3	1.3	.3	
4	2.3	.7	
5	3.1	4.1	
6	4.2	9.8	
7	5.3	6.9	
8	6.2	9.2	
9	7.1	6.8	
10	8.0	14.4	
11	9.2	12.3	
12	10.1	14.9	
13	11.1	6.7	
14	12.1	4.6	
14 1/2	12.6	1.4	
15	13.2	1.7	
15 1/2	13.7	6.2	
16	14.2	3.3	
17	15.1	5.0	
18	16.0	26.1	
19	17.0	47.1	
20	18.0	48.5	
21	19.0	30.5	
22	20.1	32.4	
23	21.0	30.9	.1
24	22.0	20.1	.1
25	23.1	18.7	.2

TRIAL 33

Roto-rod No.	Distance from Release	Dosage* Obs.	Dosage* Cal.
1	0.1 mi.	1.0	
2	1.0	.9	
3	2.0	.6	
4	3.1	3.4	
5	3.9	5.9	
6	5.1	4.1	
7	6.3	3.0	
8	7.2	2.1	.2
9	8.1	2.1	.7
10	9.1	2.6	1.7
11	10.4	2.3	3.5
12	11.4	2.4	5.2
13	12.3	1.6	6.7
14	13.4	.9	8.4
14 1/2	13.9	1.0	9.2
15	14.4	.9	9.8
15 1/2	14.8	6.1	10.3
16	15.3	2.9	10.8
17	16.3	5.5	12.0
18	17.3	10.2	12.8
19	18.3	18.4	13.5
20	19.3	22.3	14.1
21	20.4	18.7	14.5
22	21.3	16.2	14.8
23	22.2	22.0	14.9
24	23.2	19.7	15.1
25	24.3	20.7	15.1

Rotorod No. 15 - Top of Ridge

*Dosage in particles-min/liter

Effective source strength 3.64×10^9 particles/meter

DOSAGES

NEVADA

TRIAL 34

Roto-rod No.	Distance from Release	Dosage* Obs.	Dosage* Cal.
1	-0.8 mi.	.4	
2	0.1	.4	
3	1.1	.1	
4	2.2	.2	
5	3.0	.1	
6	4.1	.5	
7	5.3	.4	.8
8	6.2	.3	3.3
9	7.2	.6	8.2
10	8.2	.6	14.4
11	9.5	.2	22.4
12	10.4	.2	27.4
13	11.4	.4	31.7
14	12.5	.5	35.8
14 1/2	12.9	.5	36.7
15	13.5	1.0	38.0
15 1/2	13.9	.2	38.7
16	14.4	.4	39.5
17	15.4	.2	40.6
18	16.4	.2	41.3
19	17.4	.4	41.6
20	18.4	.7	41.5
21	19.5	.4	41.1
22	20.4	.5	40.9
23	21.4	.2	40.4
24	22.3	.6	39.6
25	23.5	.2	38.8

TRIAL 35

Roto-rod No.	Distance from Release	Dosage* Obs.	Dosage* Cal.
1	-5.1 mi.	.1	
2	-4.2	.6	
3	-3.3	.1	
4	-2.3	0	
5	-1.5	.3	
6	-0.5	.1	
7	0.7	.1	
8	1.4	0	
9	2.3	.3	
10	3.2	.3	
11	4.3	.4	
12	5.2	.5	
13	6.0	.8	
14	7.1	14.6	
14 1/2	7.7	13.4	
15	8.2	10.8	
15 1/2	8.7	6.2	
16	9.2	13.0	
17	10.1	14.5	
18	11.0	19.3	
19	11.9	23.2	
20	12.9	21.1	.1
21	14.0	11.0	.2
22	14.9	12.0	.3
23	15.8	12.9	.5
24	16.8	24.3	.8
25	17.8	13.3	1.1

Rotorod No. 15 - Top of Ridge

*Dosage in particles-min/liter

Effective source strength 3.64×10^9 particles/meter

DOSAGES

NEVADA

TRIAL 36

Roto-rod No.	Distance from Release	Dosage* Obs.	Cal.
1	-1.7 mi.	.2	
2	-0.9	0	
3	0.1	0	
4	1.0	0	
5	1.9	.1	
6	2.9	0	
7	4.0	.2	
8	4.8	.3	
9	5.7	.1	
10	6.6	.6	
11	7.7	.7	
12	8.5	1.6	
13	9.5	7.3	
14	10.4	4.7	
14 1/2	11.0	2.1	
15	11.5	1.7	
15 1/2	12.0	4.4	
16	12.6	6.3	
17	13.5	7.3	.1
18	14.4	7.0	.2
19	15.2	15.5	.3
20	16.3	14.1	.5
21	17.3	16.0	.8
22	18.3	13.5	1.2
23	19.2	7.0	1.5
24	20.2	9.7	2.0
25	21.2	9.1	2.5

Rotorod No. 15 - Top of Ridge

*Dosage in particles-min/liter

Effective source strength 3.64×10^9 particles/meter